Inorganic Chemistry

Article

pubs.acs.org/IC

# Syntheses, X-ray Crystal Structures, and Optical, Fluorescence, and Nonlinear Optical Characterizations of Diphenylphosphino-Substituted Bithiophenes

Qun Zhao,*[,†] Jason L. Freeman,[†] Jianwei Wang,[‡] Yuanli Zhang,[‡] Tracy P. Hamilton,[†] Christopher M. Lawson,[‡] and Gary M. Gray*[,†]

[†]Department of Chemistry, University of Alabama, 201 Chemistry Building, 901 14th Street South, Birmingham, Alabama 35294-1240, United States

[‡]Department of Physics, University of Alabama, CH 310, 1530 Third Avenue South, Birmingham, Alabama, 35294-1170

Supporting Information

**ABSTRACT:** A series of bithiophene derivatives that are either symmetrically disubstituted with two $Ph_2(X)P$ groups (X = O, S, Se) or monosubstituted with one $Ph_2(X)P$ group (X = O, S, Se) and an organic functional group (H, CHO, $CH_2OH$, $CO_2Me$) have been synthesized. The X-ray crystal structures of $Ph_2(Se)P(C_4H_2S)_2P(Se)Ph_2$, $Ph_2(O)P(C_4H_2S)_2H$, $Ph_2(S)P(C_4H_2S)_2H$, and $Ph_2(O)P(C_4H_2S)_2CH_2OH$ exhibit very different solid-state structures depending on the type of intermolecular $\pi-\pi$ interactions that occur. The compounds have been characterized by electronic absorption and fluorescence studies. Of particular interest is that the quantum yields of $Ph_2(O)P(C_4H_2S)_2H$, $Ph_2(O)P(C_4H_2S)_2P(O)Ph_2$, $Ph_2(O)P(C_4H_2S)_2CO_2Me$, and $Ph_2(O)P(C_4H_2S)_2CH_2OH$ are significantly larger than that of bithiophene (factors of 13, 14, 14, and 22, respectively). This behavior is quite different from that of analogously substituted terthiophenes in which substitution results in only modest increases in the quantum yields over that of terthiophene (factors of 0.94, 2.7, 1.3, and 1.5, respectively). DFT studies of the emission process suggest that modifying the $Ph_2(X)P$ group affects both the fluorescence and nonradiative rate constants while modifications of the organic substituents primarily affect the nonradiative rate constants. The higher quantum yields of the substituted bithiophenes make them promising for application in organic light-emitting devices (OLED). The optical power limiting (OPL) performances of these $Ph_2(X)P$-substituted bithiophenes were evaluated by nonlinear transmission measurements in the violet-blue spectral region (430−480 nm) with picosecond laser pulses. The OPL performances are enhanced by heavier X groups and when by higher solubilities. Saturated chloroform solutions of $Ph_2(O)P(C_4H_2S)_2H$ and $Ph_2(S)P(C_4H_2S)_2H$ exhibit significantly stronger nonlinear absorption than any previously reported compounds and are promising candidates for use in broadband optical power limiters.

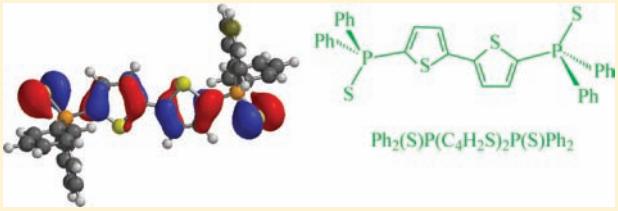


## INTRODUCTION

Materials exhibiting strong third-order nonlinear optical (NLO) absorptions have attracted considerable interest because of their potential applications in optical switching,[1,2] three-dimensional (3D) fluorescence imaging,[3] 3D optical data storage,[4] 3D lithographic microfabrication,[5,6] and optical power limiting.[7−12] Of particular interest for many of these applications are materials exhibiting multiphoton absorption, and the development of such materials has been recently reviewed by Marder,[13−15] Belfield,[16,17] and He.[18]

For power limiting applications, compounds with strong NLO absorption in all areas of the visible spectrum[19−22] are needed, and until very recently, few NLO absorbers in the violet and blue spectral regions were known.[23] In early 2011, we reported that dichloromethane solutions of $Ph_2(X)P$-substituted terthiophenes (X = O, S, $Me^+I^-$) exhibited promising NLO absorption ranging from 450 to 532 nm with picosecond laser pulses.[24] The results were promising because the nonlinear absorption was in the blue spectral region, and both the intensity and wavelength of the NLO absorption could be tuned by changing either the X group or other substituent on the terthiophene. Nonetheless, because of the significant linear absorptions of these compounds in the blue spectral region, rather dilute dichloromethane solutions ($3.5 \times 10^{-3}$ mol/L) had to be used, which in turn resulted in relatively weak NLO absorption.

To avoid the linear absorption issues encountered with the $Ph_2(X)P$-substituted terthiophenes, we investigated closely related $Ph_2P(X)$-substituted bithiophenes because these compounds should have higher linear transmittances in the violet-blue region of interest.[25] We recently reported that saturated dichloromethane solutions of two of these compounds, $Ph_2(X)P(C_4H_2S)_2P(X)Ph_2$ (X = O (**2**), S (**3**)) (chart 1) exhibited

**Received:** June 17, 2011
**Published:** February 9, 2012

   dx.doi.org/10.1021/ic201309k | *Inorg. Chem.* 2012, 51, 2016−2030

**Chart 1. Chemical Structures of the $Ph_2(X)P$-Substituted Bithiophenes**

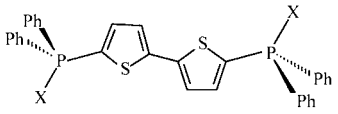

**1** X = -
**2** X = O
**3** X = S
**4** X = Se

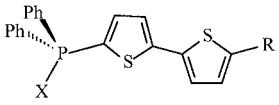

**5** X = -; R = H
**6** X = O; R = H
**7** X = S; R = H
**8** X = Se; R = H
**9** X = O; R = CHO
**10** X = O; R = $CH_2OH$
**11** X = O; R = $CO_2Me$

stronger NLO absorption than the analogously substituted terthiophenes between 420 and 480 nm.[26] Moreover, the X group has a significant effect on the nonlinear absorption with **3** exhibiting stronger NLO absorption than **2** at all wavelengths. These preliminary studies suggest that NLO absorptions may be due to two-photon absorption with ps laser pulses.

In addition to their promising nonlinear optical properties, the fluorescence spectra of the $Ph_2P(X)$-substituted terthiophenes and bithiophenes are also of great interest. Our previous studies showed that the $Ph_2P(O)$-substituted terthiophenes exhibit strong fluorescence emission and wide band gaps, making them promising candidates as materials for blue organic light emitting devices (OLED).[24] The parent compounds, $Ph_2P$-substitued bithiophenes and terthiophenes, were reported to have quite different ground and first singlet excited states,[25] but it is unknown whether the $Ph_2P(X)$-substitution could have different effects on the fluorescent properties in these two classes of compounds. In our preliminary study the substituted bithiophene **2** exhibits strong fluorescence in the violet-blue spectral region,[26] which was surprising because the quantum yield of bithiophene is only 20% of that of terthiophene. However, a systematic investigation of the influence of variation of the $Ph_2P(X)$ groups and other $\alpha$-substituents on the fluorescent properties of the substituted bithiophenes is necessary to develop compounds with optimal fluorescent properties.

The NLO studies described above suggest that the optical limiting performances of the NLO absorbers could be further improved either by attaching even heavier chalcogens to the $Ph_2P(X)$ substituent or by increasing the solubilities of the molecules. To test these possibilities and to gain more insight into the factors that might affect the fluorescent properties of the $Ph_2P(X)$-substituted bithiophenes, we have synthesized and characterized a bithiophene derivative that is symmetrically disubstituted with two $Ph_2(Se)P$ groups, **4**, and bithiophene derivatives that are substituted with one $Ph_2(X)P$ group (X = O (**6**), S (**7**), Se (**8**)) or with one $Ph_2(O)P$ group and an organic group (CHO (**9**), $CH_2OH$ (**10**), $CO_2Me$ (**11**)) at the 5- and 5′-positions (Chart 1). Absorption and fluorescence spectra, NLO absorptions of solutions of these compounds in the violet-blue spectral region and structure–property relations for the linear and NLO properties of these compounds are reported. To gain additional insight into these structure–property relationships, density functional computational studies have been carried out, and the X-ray crystal structures of the compounds, **4**, **6**, **7**, and **10** have also been determined.

## EXPERIMENTAL SECTION

**Materials and Spectroscopic Characterization.** All reagents were reagent grade quality, purchased commercially, and used as such unless otherwise indicated. Urea hydrogen peroxide (1 g tablets) was purchased from Acros Organics. Tetrahydrofuran (THF) was dried over $MgSO_4$, refluxed over sodium/benzophenone, and then distilled prior to use. Compound **1** was made by a modification of a literature procedure.[28] Compounds **2** and **3** were prepared using our previously reported procedures.[25]

One-dimensional multinuclear $^1H$ NMR, $^{31}P\{^1H\}$ NMR, and $^{13}C\{^1H\}$ NMR spectra were recorded on a Bruker DRX-400 NMR spectrometer. The $^{31}P\{^1H\}$ NMR spectra were referenced to external 85% phosphoric acid ($H_3PO_4$) in a coaxial tube that also contained chloroform-*d*. The $^1H$ NMR and $^{13}C\{^1H\}$ NMR spectra were referenced to internal tetramethylsilane (TMS). Two-dimensional COSY (correlated spectroscopy), HSQC (heteronuclear single quantum coherence spectroscopy), and HMBC (heteronuclear multiple bond correlation) were recorded on a Bruker DPX-300 NMR spectrometer. Microanalyses for % C, H, and N were performed by Atlantic Microlab, Inc.

**5,5′-Bis(diphenylselenidophosphino)-2, 2′-bithiophene, $Ph_2(Se)P(C_4H_2S)_2P(Se)Ph_2$, 4.** Excess gray selenium (0.22 g, 2.8 mmol) was added to a solution of compound **1** (0.50 g, 0.94 mmol) in dry $CH_2Cl_2$ (30 mL), and the mixture was stirred at room temperature overnight. The resulting solution was evaporated under reduced pressure to give a residue, which was purified by column chromatography on silica gel (1:1 $CHCl_3$/hexanes) to yield analytically pure **4** as a pale yellow crystalline solid (0.58 g, 89%). $^{31}P\{^1H\}$ NMR ($CDCl_3$): 23.250 (s), 23.251 (d, $|^1J_{PSe}|$ 739 Hz). $^1H$ NMR ($CDCl_3$): 7.80–7.74 (m, 8H, $H_{Ph\text{-}o}$), 7.54–7.44 (m, 12H, $H_{Ph\text{-}p}$ and $H_{Ph\text{-}m}$), 7.31 (dd, 2H, $|^3J_{PH}|$ 8.3 Hz, $|^3J_{HH}|$ 3.8 Hz, $H_{Th\text{-}4}$), 7.24 (dd, 2H, $|^4J_{PH}|$ 1.8 Hz, $|^3J_{HH}|$ 3.8 Hz, $H_{Th\text{-}3}$). $^{13}C\{^1H\}$ NMR ($CDCl_3$): $\delta$ 144.98 (d, $|^3J_{CP}|$ 7 Hz, $C_{Th\text{-}2}$), 138.20 (d, $|^2J_{CP}|$ 8 Hz, $C_{Th\text{-}4}$), 134.74 (d, $|^1J_{CP}|$ 82 Hz, $C_{Th\text{-}5}$), 132.20 (d, $|^1J_{CP}|$ 81 Hz, $C_{Ph\text{-}i}$), 132.28 (d, $|^2J_{CP}|$ 11 Hz, $C_{Ph\text{-}o}$ and $C_{Ph\text{-}p}$), 128.83 (d, $|^3J_{CP}|$ 14 Hz, $C_{Ph\text{-}m}$), 126.07 (d, $|^3J_{CP}|$ 13 Hz, $C_{Th\text{-}3}$). UV–vis ($CHCl_3$): $\lambda_{max}$/nm ($\varepsilon$/dm$^3$·mol$^{-1}$·cm$^{-1}$) = 348 ($2.25 \times 10^4$). Anal. Calcd for $[C_{32}H_{24}P_2S_2Se_2]$: C, 55.50; H, 3.49. Found: C, 55.11; H, 3.45.

**5-(Diphenylphosphino)-2,2′-bithiophene, $Ph_2P(C_4H_2S)_2H$, 5.** Although the synthesis of **5** was reported in the literature,[28] we prepared **5** by a different method. A solution of 2,2′-bithiophene (2.0 g, 12 mmol) in dry THF (50 mL) was cooled in an acetone/dry ice slush bath (−78 °C), and *n*-BuLi (1.6 *M* in hexane, 7.5 mL, 12 mmol) was added dropwise to the solution. The addition was completed in ~20 min, during which time the color of the solution darkened to a deep green. The resulting solution was warmed to room temperature for 0.5 h and then cooled again in an ice bath (0 °C). Then $PPh_2Cl$ (2.5 mL, 13 mmol) was added dropwise with a syringe. The reaction mixture was gradually brought to room temperature and stirred for 2 h. A few drops of degassed water were added to decompose any remaining lithium salt, and then the solvent was removed in vacuo, yielding a viscous oily residue. This residue was purified by column chromatography under a nitrogen atmosphere by degassing the eluent (hexanes–diethyl ether, 10:1) and the silica slurry. The resulting crude product was further purified by multiple precipitations from $CH_2Cl_2$ with hexanes yielding a colorless oil (3.2 g, 76%). $^{31}P\{^1H\}$ NMR ($CDCl_3$): −17.62 (s).

**5-Diphenyloxophosphino-2,2′-bithiophene, $Ph_2(O)P(C_4H_2S)_2H$, 6.** A 30% aqueous solution of hydrogen peroxide (1.5 mL) was added to a solution of **5** (1.00 g, 2.85 mmol) in acetone/$CH_2Cl_2$ (1:1, 50 mL). The reaction mixture was stirred at room temperature overnight and then was evaporated to dryness under reduced pressure. The residue was purified by column chromatography on silica gel (1:1 hexanes-ethyl acetate) to yield analytically pure **6** as a white crystalline solid (0.83 g, 81%). $^{31}P\{^1H\}$ NMR ($CDCl_3$): 22.64 (s). $^1H$ NMR ($CDCl_3$): 7.80–7.74 (m, 4H, $H_{Ph\text{-}o}$), 7.58–7.46 (m, 6H, $H_{Ph\text{-}p}$ and $H_{Ph\text{-}m}$), 7.34 (dd, 1H, $|^3J_{PH}|$ 7.5 Hz, $|^3J_{HH}|$ 3.7 Hz, $H_{Th\text{-}4}$), 7.25 (d, 1H, $|^3J_{HH}|$ 5.1 Hz, $H_{Th\text{-}5'}$), 7.22–7.20 (m, 2H, $H_{Th\text{-}3}$ and $H_{Th\text{-}3'}$), 7.00 (dd, 1H, $|^3J_{HH}|$ 5.1 Hz, $|^3J_{HH}|$ 3.7 Hz, $H_{Th\text{-}4'}$). $^{13}C\{^1H\}$ NMR ($CDCl_3$): $\delta$ 146.16 (d, $|^3J_{CP}|$ 5 Hz, $C_{Th\text{-}2}$), 137.73 (d, $|^2J_{CP}|$ 9 Hz, $C_{Th\text{-}4}$), 135.88 (d, $|^4J_{CP}|$ 2 Hz, $C_{Th\text{-}2'}$), 132.77 (d, $|^1J_{CP}|$ 110 Hz, $C_{Ph\text{-}i}$), 132.12 (d, $|^1J_{CP}|$ 111 Hz, $C_{Th\text{-}5}$), 132.37 (d, $|^4J_{CP}|$ 3 Hz, $C_{Ph\text{-}p}$), 131.87 (d, $|^2J_{CP}|$ 11 Hz, $C_{Ph\text{-}o}$), 128.66 (d, $|^3J_{CP}|$ 13 Hz, $C_{Ph\text{-}m}$), 128.17 (s, $C_{Th\text{-}4'}$), 126.08 (s, $C_{Th\text{-}5'}$), 125.32 (s, $C_{Th\text{-}3'}$), 124.59 (d, $|^3J_{CP}|$ 13 Hz, $C_{Th\text{-}3}$). UV–vis


dx.doi.org/10.1021/ic201309k | Inorg. Chem. 2012, 51, 2016–2030

**Table 1. Data Collection Parameters for X-ray Structure Determination**

| | 4 | 6 | 7 | 10 |
|---|---|---|---|---|
| CCDC number | 823524 | 823525 | 823522 | 823523 |
| empirical formula | $C_{32}H_{24}P_2S_2Se_2$ | $C_{20}H_{15}OPS_2$ | $C_{20}H_{15}PS_3$ | $C_{21}H_{17}O_2PS_2$ |
| formula weight | 692.49 | 366.41 | 382.47 | 396.44 |
| wavelength (Å) | 0.71073 | 0.71073 | 0.71073 | 0.71073 |
| crystal system | triclinic | triclinic | triclinic | monoclinic |
| space group | $P\bar{1}$ | $P\bar{1}$ | $P\bar{1}$ | $P2(1)/n$ |
| $a$ (Å) | 9.565(2) | 6.2348(12) | 9.4687(19) | 9.4366(19) |
| $b$ (Å) | 9.6172(19) | 8.5970(17) | 9.6133(19) | 11.474(2) |
| $c$ (Å) | 16.930(3) | 17.503(4) | 21.395(4) | 17.698(4) |
| $\alpha$ (deg) | 85.68(3) | 79.99(3) | 82.00(3) | 90° |
| $\beta$ (deg) | 74.46(3) | 83.97(3) | 80.68(3) | 102.12(3) |
| $\gamma$ (deg) | 78.10(3) | 70.75(3) | 78.17(3) | 90° |
| volume (Å$^3$) | 1467.9(5) | 871.1(3) | 1869.6(6) | 1873.6(6) |
| $Z$ | 2 | 2 | 4 | 4 |
| density (calculated) (mg/m$^3$) | 1.567 | 1.397 | 1.359 | 1.405 |
| abs coeff (mm$^{-1}$) | 2.791 | 0.401 | 0.480 | 0.382 |
| $F$(000) | 692 | 380 | 792 | 824 |
| cryst size (mm) | 0.9 × 0.6 × 0.3 | 0.6 × 0.3 × 0.2 | 0.5 × 0.4 × 0.3 | 0.6 × 0.4 × 0.4 |
| $\theta$ range for data collection (deg) | 2.16−24.97 | 2.37−24.97 | 2.18−24.97 | 2.13−24.99 |
| index ranges | $-11 \le h \le 0$ | $-7 \le h \le 1$ | $-11 \le h \le 11$ | $-11 \le h \le 11$ |
| | $-11 \le k \le 11$ | $-10 \le k \le 10$ | $-1 \le k \le 11$ | $-1 \le k \le 13$ |
| | $-20 \le l \le 19$ | $-20 \le l \le 20$ | $-25 \le l \le 25$ | $-1 \le l \le 21$ |
| reflns collected | 5517 | 3988 | 7872 | 4036 |
| independent reflns | 5176 | 3069 | 6591 | 3299 |
| | [$R$(int) = 0.0206] | [$R$(int) = 0.0350] | [$R$(int) = 0.0402] | [$R$(int) = 0.0242] |
| completeness to $\theta$ = 22.48° | 100.0% | 100.0% | 100.0% | 99.9% |
| abs correction | $\psi$-scan | none | none | none |
| max. and min transmission | 1.0000 and 0.3596 | | | |
| refinement method | full-matrix least-squares on $F^2$ | full-matrix least-squares on $F^2$ | full-matrix least-squares on $F^2$ | full-matrix least-squares on $F^2$ |
| data/restraints/params | 5176/0/344 | 3069/0/218 | 6591/150/470 | 3299/0/240 |
| GOF on $F^2$ | 1.060 | 1.053 | 1.059 | 1.091 |
| final R indices [$I > 2\sigma(I)$] | R1 = 0.0458 | R1 = 0.0537 | R1 = 0.0480 | R1 = 0.0410 |
| | wR2 = 0.1199 | wR2 = 0.1578 | wR2 = 0.1291 | wR2 = 0.1106 |
| R indices (all data) | R1 = 0.0700 | R1 = 0.0658 | R1 = 0.0698 | R1 = 0.0557 |
| | wR2 = 0.1335 | wR2 = 0.1690 | wR2 = 0.1410 | wR2 = 0.1233 |
| largest diff. peak/hole (eÅ$^{-3}$) | 0.694 and −0.892 | 0.682 and −0.522 | 0.329 and −0.494 | 0.467 and −0.279 |

($CHCl_3$): $\lambda_{max}$/nm ($\varepsilon$/dm$^3$·mol$^{-1}$·cm$^{-1}$) = 321 (1.75 × 10$^4$). Anal. Calcd for [$C_{20}H_{15}OPS_2$]: C, 65.55; H, 4.13. Found: C, 65.62; H, 3.95.

**5-Diphenylsulfidophosphino-2,2′-bithiophene, $Ph_2(S)P(C_4H_2S)_2H$, 7.** Elemental sulfur (0.16 g, 5.0 mmol) was added to a solution of **5** (1.0 g, 2.9 mmol) in $CH_2Cl_2$ (50 mL). The reaction mixture was stirred at room temperature overnight and then was evaporated under reduced pressure. The residue was purified by column chromatography on silica gel. First, the excess sulfur was removed by elution with hexanes, and then elution with 10:1 hexanes/$Et_2O$ yielded analytically pure **7** as a white crystalline solid (0.95 g, 87%). $^{31}P\{^1H\}$ NMR ($CDCl_3$): 34.68 (s). $^1H$ NMR ($CDCl_3$): 7.83−7.77 (m, 4H, $H_{Ph\text{-}o}$), 7.54−7.44 (m, 6H, $H_{Ph\text{-}p}$ and $H_{Ph\text{-}m}$), 7.322 (dd, 1H, $|^3J_{PH}|$ 8.3 Hz, $|^3J_{HH}|$ 3.8 Hz, $H_{Th\text{-}4}$), 7.26 (d, 1H, $|^3J_{HH}|$ 5.1 Hz, $H_{Th\text{-}5'}$), 7.21−7.17 (m, 2H, $H_{Th\text{-}3}$ and $H_{Th\text{-}3'}$), 7.01−6.99 (m, 1H, $H_{Th\text{-}4'}$). $^{13}C\{^1H\}$ NMR ($CDCl_3$): $\delta$ 146.68 (d, $|^3J_{CP}|$ 5 Hz, $C_{Th\text{-}2}$), 137.90 (d, $|^2J_{CP}|$ 9 Hz, $C_{Th\text{-}4}$), 136.10 (s, $C_{Th\text{-}2'}$), 133.62 (d, $|^1J_{CP}|$ 89 Hz, $C_{Th\text{-}5}$), 133.61 (d, $|^1J_{CP}|$ 90 Hz, $C_{Ph\text{-}i}$), 132.09 (s, $C_{Ph\text{-}p}$), 131.99 (d, $|^2J_{CP}|$ 11 Hz, $C_{Ph\text{-}o}$), 128.80 (d, $|^3J_{CP}|$ 13 Hz, $C_{Ph\text{-}m}$), 128.30 (s, $C_{Th\text{-}4'}$), 126.18 (s, $C_{Th\text{-}5'}$), 125.38 (s, $C_{Th\text{-}3'}$), 124.70 (d, $|^3J_{CP}|$ 13 Hz, $C_{Th\text{-}3}$). UV−vis ($CHCl_3$): $\lambda_{max}$/nm ($\varepsilon$/dm$^3$·mol$^{-1}$·cm$^{-1}$) = 328 (2.01 × 10$^4$). Anal. Calcd for [$C_{20}H_{15}PS_5$]: C, 62.80; H, 3.95. Found: C, 62.96; H, 3.78.

**5-Diphenylselenidophosphino-2,2′-bithiophene, $Ph_2(Se)P(C_4H_2S)_2H$, 8.** Gray selenium (0.12 g, 1.5 mmol) was added to a solution of **5** (0.45 g, 1.3 mmol) in $CH_2Cl_2$ (30 mL). The reaction mixture was stirred at room temperature overnight and then was evaporated under reduced pressure. The residue was purified by column chromatography on silica gel (1:1 hexanes/$Et_2O$) yielding analytically pure **8** as a white crystalline solid (0.45 g, 82%). $^{31}P\{^1H\}$ NMR ($CDCl_3$): 23.28 (s), 23.24 (d, $|^1J_{PSe}|$ 735 Hz). $^1H$ NMR ($CDCl_3$): 7.83−7.77 (m, 4H, $H_{Ph\text{-}o}$), 7.54−7.44 (m, 6H, $H_{Ph\text{-}p}$ and $H_{Ph\text{-}m}$), 7.33 (dd, 1H, $|^3J_{PH}|$ 8.6 Hz, $|^3J_{HH}|$ 3.8 Hz, $H_{Th\text{-}4}$), 7.27 (d, 1H, $|^3J_{HH}|$ 5.1 Hz, $H_{Th\text{-}5'}$), 7.22−7.20 (m, 2H, $H_{Th\text{-}3}$ and $H_{Th\text{-}3'}$), 7.01 (dd, 1H, $|^3J_{HH}|$ 5.1 Hz, $|^3J_{HH}|$ 3.8 Hz, $H_{Th\text{-}4'}$). $^{13}C\{^1H\}$ NMR ($CDCl_3$): $\delta$ 146.96 (d, $|^3J_{CP}|$ 5 Hz, $C_{Th\text{-}2}$), 138.41 (d, $|^2J_{CP}|$ 9 Hz, $C_{Th\text{-}4}$), 136.08 (s, $C_{Th\text{-}2'}$), 132.62 (d, $|^1J_{CP}|$ 82 Hz, $C_{Ph\text{-}i}$), 132.36 (d, $|^1J_{CP}|$ 84 Hz, $C_{Th\text{-}5}$), 132.36 (d, $|^2J_{CP}|$ 12 Hz, $C_{Ph\text{-}o}$), 132.06 (d, $|^4J_{CP}|$ 3 Hz, $C_{Ph\text{-}p}$), 128.78 (d, $|^3J_{CP}|$ 13 Hz, $C_{Ph\text{-}m}$), 128.28 (s, $C_{Th\text{-}4'}$), 126.20 (s, $C_{Th\text{-}5'}$), 125.40 (s, $C_{Th\text{-}3'}$), 124.74 (d, $|^3J_{CP}|$ 13 Hz, $C_{Th\text{-}3}$). UV−vis ($CHCl_3$): $\lambda_{max}$/nm ($\varepsilon$/dm$^3$·mol$^{-1}$·cm$^{-1}$) = 329 (1.92 × 10$^4$). Anal. Calcd for [$C_{20}H_{15}PS_2Se$]: C, 55.94; H, 3.52. Found: C, 55.93; H, 3.42.

**5-Diphenyloxophosphino-2, 2′-bithiophene-5′-carbaldehyde, $Ph_2(O)P(C_4H_2S)_2CHO$, 9.** A solution of **6** (1.00 g, 2.73 mmol) in anhydrous DMF (2.00 mL) stirred as $POCl_3$ (1.25 mL, 13.6 mmol) was added dropwise. The reaction mixture was heated at 80 °C under nitrogen for 36 h and then was poured slowly into 100 mL of saturated aqueous sodium acetate solution. This mixture was stirred for 2 h, and then the organic layer was diluted with $CH_2Cl_2$, separated, and washed with water. After evaporation of the solvents, the solid residue was purified with silica gel flash chromatography (ethyl acetate) to yield analytically pure **9** as a yellow product (0.92 g, 83%). $^{31}P\{^1H\}$ NMR ($CDCl_3$): 22.53 (s). $^1H$ NMR ($CDCl_3$): 9.87 (s, 1H, $H_{CHO}$), 7.80−7.74 (m, 4H, $H_{Ph\text{-}o}$), 7.68 (d, 1H,


dx.doi.org/10.1021/ic201309k | Inorg. Chem. 2012, 51, 2016−2030

$|^3J_{HH}|$ 3.9 Hz, $H_{Th\text{-}3'}$ or $H_{Th\text{-}4'}$), 7.61−7.57 (m, 2H, $H_{Ph\text{-}p}$), 7.53−7.48 (m, 4H, $H_{Ph\text{-}m}$), 7.40−7.38 (m, 2H, $H_{Th\text{-}3}$ or $H_{Th\text{-}4}$), 7.29 (d, 1H, $|^3J_{HH}|$ 3.9 Hz, $H_{Th\text{-}3'}$ or $H_{Th\text{-}4'}$). $^{13}C\{^1H\}$ NMR ($CDCl_3$): $\delta$ 182.69 (s, $C_{CHO}$), 145.17 (s, $C_{Th\text{-}2'}$ or $C_{Th\text{-}5'}$), 144.24 (d, $|^3J_{CP}|$ 6 Hz, $C_{Th\text{-}2}$), 143.19 (s, $C_{Th\text{-}2'}$ or $C_{Th\text{-}5'}$), 137.72 (d, $|^2J_{CP}|$ 9 Hz, $C_{Th\text{-}4}$ or $C_{Th\text{-}3}$), 137.19 (s, $C_{Th\text{-}3'}$ or $C_{Th\text{-}4'}$), 135.72 (d, $|^1J_{CP}|$ 108 Hz, $C_{Th\text{-}5}$), 132.39 (d, $|^1J_{CP}|$ 111 Hz, $C_{Ph\text{-}i}$), 132.65 (d, $|^4J_{CP}|$ 3 Hz, $C_{Ph\text{-}p}$), 131.91 (d, $|^2J_{CP}|$ 11 Hz, $C_{Ph\text{-}o}$), 128.83 (d, $|^3J_{CP}|$ 13 Hz, $C_{Ph\text{-}m}$), 126.86 (d, $|^2J_{CP}|$ 13 Hz, $C_{Th\text{-}4}$ or $C_{Th\text{-}3}$), 125.84 (s, $C_{Th\text{-}3'}$ or $C_{Th\text{-}4'}$). UV−vis ($CHCl_3$): $\lambda_{max}$/nm ($\varepsilon$/dm$^3$·mol$^{-1}$·cm$^{-1}$) = 356 ($2.63 \times 10^4$). Anal. Calcd for $[C_{21}H_{15}O_2PS_2]$: C, 63.94; H, 3.83. Found: C, 63.79; H, 3.67.

**5′-Hydroxymethyl-5-diphenyloxophosphino-2,2′-bithiophene, $Ph_2(O)P(C_4H_2S)_2CH_2OH$, 10.** Sodium borohydride (0.080 g, 2.1 mmol) was added to a solution of **9** (0.40 g, 1.01 mmol) in dry THF (10 mL) under nitrogen at ambient temperature. The reaction mixture was stirred overnight, and then, the THF was evaporated. The resultant residue was recrystallized from ethyl acetate affording **10** as an analytically pure white crystalline powder (0.32 g, 80%). $^{31}P\{^1H\}$ NMR ($CDCl_3$): 23.24 (s). $^1H$ NMR ($CDCl_3$): 7.76−7.71 (m, 4H, $H_{Ph\text{-}o}$), 7.59−7.55 (m, 2H, $H_{Ph\text{-}p}$), 7.50−7.46 (m, 4H, $H_{Ph\text{-}m}$), 7.23 (dd, 1H, $|^3J_{PH}|$ 7.6 Hz, $|^3J_{HH}|$ 3.8 Hz, $H_{Th\text{-}4}$), 7.10−7.08 (m, 1H, $H_{Th\text{-}3}$), 6.99 (d, 1H, $|^3J_{HH}|$ 3.6 Hz, $H_{Th\text{-}3'}$), 6.82 (d, 1H, $|^3J_{HH}|$ 3.6 Hz, $H_{Th\text{-}4'}$), 4.78 (s, 2H, $H_{CH2}$), 3.68 (br, 1H, $H_{OH}$). $^{13}C\{^1H\}$ NMR ($CDCl_3$): $\delta$ 146.53 (d, $|^3J_{CP}|$ 5 Hz, $C_{Th\text{-}2}$), 146.42 (s, $C_{Th\text{-}2'}$ or $C_{Th\text{-}5'}$), 137.74 (d, $|^2J_{CP}|$ 10 Hz, $C_{Th\text{-}4}$), 135.17 (s, $C_{Th\text{-}2'}$ or $C_{Th\text{-}5'}$), 133.17 (d, $|^1J_{CP}|$ Hz, $C_{Ph\text{-}i}$), 132.33 (d, $|^4J_{CP}|$ 2 Hz, $C_{Ph\text{-}p}$), 131.79 (d, $|^2J_{CP}|$ 11 Hz, $C_{Ph\text{-}o}$), 131.26 (d, $|^1J_{CP}|$ 112 Hz, $C_{Th\text{-}5}$), 128.59 (d, $|^3J_{CP}|$ 13 Hz, $C_{Ph\text{-}m}$), 125.51 (s, $C_{Th\text{-}3'}$ or $C_{Th\text{-}4'}$), 124.87 (s, $C_{Th\text{-}3'}$ or $C_{Th\text{-}4'}$), 124.14 (d, $|^3J_{CP}|$ 13 Hz, $C_{Th\text{-}3}$), 59.81 (s, $C_{CH2}$). UV−vis ($CHCl_3$): $\lambda_{max}$/nm ($\varepsilon$/dm$^3$·mol$^{-1}$·cm$^{-1}$) = 329 ($1.98 \times 10^4$). Anal. Calcd for $[C_{21}H_{17}O_2PS_2]$: C, 63.62; H, 4.32. Found: C, 63.85; H, 4.22.

**Methyl 5-(Diphenyloxophosphino)-2,2′-bithiophene-5′-carboxylate, $Ph_2(O)P(C_4H_2S)_2CO_2Me$, 11.** Molecular iodine $I_2$ (3 equiv) and $K_2CO_3$ (3 equiv) were added to a solution of **10** (0.21 mg, 0.54 mmol) in dry $CH_3OH$ (0.5 mL) and dry $ClCH_2CH_2Cl$ (2 mL) under a nitrogen atmosphere. The reaction mixture was refluxed at 70 °C for 20 h before it was quenched with saturated aquaous $Na_2SO_3$ at 0 °C. This mixture was extracted with $CH_2Cl_2$; the organic layer was dried and evaporated to dryness, and the crude product was purified with flash chromatography on silica gel (ethyl acetate) to yield analytically pure product as a white crystalline powder (0.18 mg, 80%). $^{31}P\{^1H\}$ NMR ($CDCl_3$): 22.55 (s). $^1H$ NMR ($CDCl_3$): 7.80−7.74 (m, 4H, $H_{Ph\text{-}o}$), 7.68 (d, 1H, $|^3J_{HH}|$ 4.0 Hz, $H_{Th\text{-}4'}$), 7.59−7.56 (m, 2H, $H_{Ph\text{-}p}$), 7.52−7.48 (m, 4H, $H_{Ph\text{-}m}$), 7.38 (dd, 1H, $|^3J_{PH}|$ 7.3 Hz, $|^3J_{HH}|$ 3.7 Hz, $H_{Th\text{-}4}$), 7.32 (dd, 1H, $|^3J_{HH}|$ 3.8 Hz, $|^4J_{PH}|$ 1.9 Hz, $H_{Th\text{-}3}$), 7.18 (d, 1H, $|^3J_{HH}|$ 4.0 Hz, $H_{Th\text{-}3'}$), 3.88 (s, 3H, $H_{CH3}$). $^{13}C\{^1H\}$ NMR ($CDCl_3$): $\delta$ 162.32 (s, $C_{Th\text{-}2'}$ or $C_{Th\text{-}5'}$), 144.68 (d, $|^4J_{CP}|$ 6 Hz, $C_{Th\text{-}2}$), 142.4 (s, $C_{Th\text{-}2'}$ or $C_{Th\text{-}5'}$), 137.69 (d, $|^2J_{CP}|$ 9 Hz, $C_{Th\text{-}4}$), 134.54 (d, $|^1J_{CP}|$ 109 Hz, $C_{Th\text{-}5}$), 134.33 (s, $C_{Th\text{-}4'}$), 133.18 (d, $|^1J_{CP}|$ 15 Hz, $C_{Ph\text{-}i}$), 133.55 (d, $|^4J_{CP}|$ 3 Hz, $C_{Ph\text{-}p}$), 131.90 (d, $|^2J_{CP}|$ 11 Hz, $C_{Ph\text{-}o}$), 128.77 (d, $|^3J_{CP}|$ 13 Hz, $C_{Ph\text{-}m}$), 126.05 (d, $|^3J_{CP}|$ 13 Hz, $C_{Th\text{-}3}$), 125.47 (s, $C_{Th\text{-}3'}$), 52.44 (s, $C_{CH3}$). UV−vis ($CHCl_3$): $\lambda_{max}$/nm ($\varepsilon$/dm$^3$·mol$^{-1}$·cm$^{-1}$) = 340 ($2.77 \times 10^4$). Anal. Calcd for $[C_{22}H_{17}O_3PS_2]$: C, 62.25; H, 4.04. Found: C, 62.55; H, 4.22.

**X-ray Data Collection and Solution.** Suitable single crystals of **4** (slow diffusion of $Et_2O$ into a concentrated $CH_2Cl_2$ solution), **6** (slow diffusion of hexanes into a concentrated $CH_2Cl_2$ solution), **7** (slow diffusion of hexanes into a concentrated $Et_2O$ solution), and **10** (slow evaporation of an ethyl acetate solution) were attached to glass fibers with epoxy cement and then were aligned upon an Enraf-Nonius CAD4 single-crystal diffractometer under aerobic conditions. Standard peak search and automatic indexing routines followed by least-squares fits of 25 accurately centered reflections resulted in accurate unit cell parameters. The space groups of the crystals were assigned on the basis of systematic absences and intensity statistics. All data collections were carried out using the CAD4-PC software,[29] and details of the data collections are given in Table 1. The analytical scattering factors of the complex were corrected for both $\Delta f'$ and $i\Delta f''$ components of anomalous dispersion. All data were corrected for Lorentz and polarization effects. The data for **4** was corrected for absorption using a $\psi$-scan with four reflections with $\chi \geq 80°$.

Crystallographic calculations were performed with the Siemens SHELXTL-PC program package.[30] All heavy atom positions were located using direct methods. Full-matrix refinements of the positional and anisotropic thermal parameters for all non-hydrogen atoms versus $F^2$ were carried out. All hydrogen atoms were placed in calculated positions with the appropriate molecular geometry and $\delta$(C−H) = 0.96 Å. The isotropic thermal parameter of each hydrogen atom was fixed equal to 1.2 times the $U_{eq}$ value of the atom to which it was bound. The unsubstituted thienyl group of **7** shows positional disorder with the one thienyl group being related to another via a 180° rotation about the C−C bond between the two groups. The disorder was modeled with the help of similarity restraints and rigid bond constraints. The occupancy was refined to a free-variable value of 0.610. Crystallographic data for all crystals have been deposited with the Cambridge Crystallographic Database (**4**, CCDC 823524; **6**, CCDC 823525; **7**, CCDC 823522; **10**, CCDC 823523).

**Linear Absorption and Solution Phase Fluorescence Measurements.** Linear absorption spectra for all compounds in $3.0 \times 10^{-4}$ mol/L chloroform solutions were recorded on a Varian Cary-100 UV−visible spectrophotometer in a 1-mm cuvette. Room-temperature emission spectra were measured on a Cary Eclipse Fluorometer. Each solution, in 10-mm path length quartz cell, was excited at the absorption wavelength maximum, and all the fluorescence spectra were recorded with a constant slit width of 5 nm. The optical densities at the excitation wavelengths were kept below 0.1 to avoid any inner-filter effects. All solutions were prepared using Optima grade chloroform, and the solutions were deoxygenated by bubbling $N_2$ through them for approximately five minutes. The emission quantum yields of the samples were determined by a comparative method[31] using eq 1

$$\Phi_S = \Phi_R \frac{I_S}{I_R} \frac{OD_R}{OD_S} \frac{{n_S}^2}{{n_R}^2} \quad (1)$$

where the subscripts S and R refer to the sample and reference solutions respectively, $I$ is the integrated emission intensity, OD is the optical density at the excitation wavelength, and $n$ is the refractive index of the solvent. A degassed quinine sulfate solution in 0.1 M $H_2SO_4$ ($\Phi$ = 0.53 at 350 nm excitation)[32] was the reference.

**Linear and Nonlinear Optical Transmission Measurements.** The linear transmission measurements of 1.66 mol/L chloroform solutions of compounds **6**−**8** in 1-mm cuvettes were performed on a Shimadzu UV-3101PC Spectrophotometer. The NLO transmission measurements were performed at 430, 450, and 480 nm, respectively, on the same solutions in the same cuvettes. NLO transmission measurements on **2**−**4**, which are considerably less soluble, were performed at the same wavelengths using 0.067 mol/L $CH_2Cl_2$ solutions. A wavelength tunable laser system, consisting of an EKSPLA PG401 optical parametric generator (OPG) pumped by a PL2143A/ss modelocked Nd:YAG laser with a pulse width of 27 ps and a repetition rate of 10 Hz, was used as the light source. Laser radiation energy was gradually changed by using a motorized attenuator based on a combination of a half-wave plate and a Glan-Taylor prism. Part of the laser beam was then reflected by a beam splitter to a reference detector to monitor the incident energy. The remaining beam was focused by a 500 mm lens to the center of a 1-mm sample cell (Spectrosil 21-Q-1, Starna Cells, Inc.). The diameters of the focused beams were 94, 98, and 98 $\mu$m at 430, 450, and 480 nm, respectively. The transmitted signal energy and the reference energy were monitored by two Molectron J4−09 pyroelectric joule meters.

**Computational Methods.** The ground state geometries of bithiophene ($T_2$), terthiophene ($T_3$), **2**−**3**, **6**−**7**, and **9**−**11** were optimized at the B3LYP/6-31G(d) level of theory using the Spartan '08 software package.[33] Spartan '08 was used to plot the highest occupied molecular orbital (HOMO) and the lowest unoccupied molecular orbital (LUMO). The starting geometries for **2**, **3**, **6**, **7**, and **10** were the experimental X-ray diffraction structures.[34] Optimized geometries of **9** and **11** were global minima when the sulfur atoms were anti


dx.doi.org/10.1021/ic201309k | Inorg. Chem. 2012, 51, 2016−2030

**Scheme 1. Syntheses of Derivatives of 5,5′-Bis(Diphenylphosphino)-2,2′-bithiophene (1)**

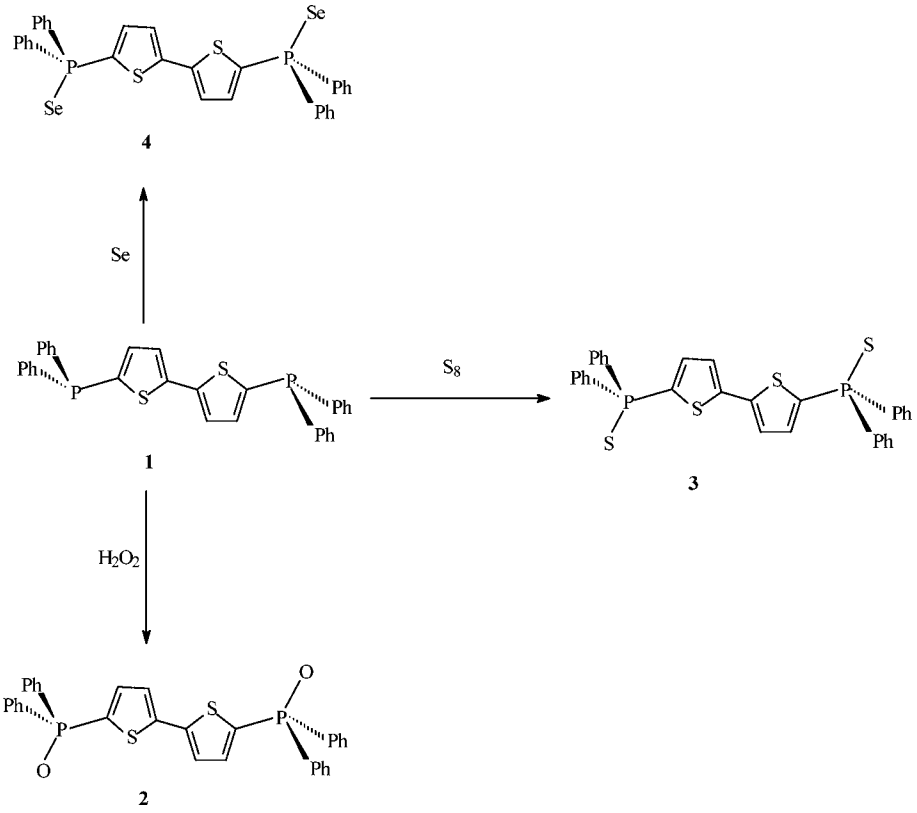


in the bithiophene moiety. Emission spectra were computed using Gaussian '03 for Windows[35] by the following procedure, which gave very good agreement between theory and experiment for closely related compounds.[36,37] The geometry of the first excited singlet state was optimized using the CIS/6-31G(d) level of theory. Time dependent DFT (based on B3LYP/6-31G(d)) was then used to calculate the emission spectra at the CIS/6-31G(d) geometry.

## RESULTS AND DISCUSSION

**Syntheses and NMR Spectroscopic Characterization.** The syntheses of the two starting materials, **1** and **5**, had quite different levels of difficulty. A modification of a literature procedure was used to prepare **1**.[28] In contrast, the synthesis of **5** was a challenging undertaking. Previous reports claimed that the selective monolithiation of bithiophene was impossible despite using a wide range of stoichiometries and reaction conditions.[28] We have found that this is not the case that **5** can be prepared by first lithiating bithiophene with *n*-butyllithium and then quenching with chlorodiphenylphosphine. The crude **5** was purified by column chromatography on silica gel under a nitrogen atmosphere and then by multiple precipitations from $CH_2Cl_2$ with hexanes until a colorless oil with a single $^{31}P\{^1H\}$ NMR resonance was obtained.

Compound **4** was synthesized by treating **1** with selenium powder and purified by column chromatography. Compounds **6**, **7**, and **8** were synthesized by treating **5** with hydrogen peroxide, elemental sulfur, and selenium powder, respectively, as shown in Schemes 1 and 2. Compound **6** could be readily functionalized with a formyl, **9**, or a hydroxymethyl group, **10**, at the 5′-position by modifications of the procedures that we previously reported for the syntheses of the terthiophene analogues.[11] The oxidative conversion of **10** with molecular iodine and $K_2CO_3$ yielded the corresponding methyl ester, **11**. To obtain **11** in high yield, it is important to use only a small amount of $CH_3OH$ (0.5 mL).[38]

All the new compounds have been characterized by $^{31}P\{^1H\}$, $^{13}C\{^1H\}$, and $^1H$ NMR spectroscopy. The $^{13}C\{^1H\}$ and $^1H$ NMR spectra were assigned using a combination of two-dimensional COSY, HSQC, and HMBC techniques. The $^{31}P\{^1H\}$ NMR resonance of **1** and **5** in $CDCl_3$ are singlets (−17.60 and −17.62 ppm, respectively) that are typical for diphenyl-phosphines with 2-thienyl substituents.[28] The $^{31}P\{^1H\}$ NMR resonances for **6**, **7**, and **8** at $\delta$ 22.64, 34.68, and 23.28 ppm, respectively, are downfield of that of **5**, while the $^{31}P\{^1H\}$ NMR resonances of **2**, **3**, and **4** at $\delta$ 22.54, 34.64, and 23.25 ppm, respectively, are downfield of that of **1**. The significantly downfield chemical shifts of the $^{31}P\{^1H\}$ NMR resonances of the $Ph_2(X)P$ (X = O, S, Se) substituted bithiophenes relative to that of the parent compounds indicate that coordination of the lone pair of phosphorus causes a significant decrease in the electron density at the phosphorus and that each substituent has a significantly different effect. The similarity of the chemical shifts of $^{31}P\{^1H\}$ NMR resonances for the disubstituted bithiophenes and the monosubstituted bithiophenes with the same $Ph_2(X)P$ groups (X = O, S, Se), indicates that the introduction of a second $Ph_2(X)P$ group at the 5′-position has no significant effect on the local magnetic field at the phosphorus atom.

The $|^1J_{PSe}|$ coupling constants for **4** (739 Hz) and **8** (735 Hz) are quite similar indicating the presence of a second $Ph_2(Se)P$ group does not affect the $^{31}P-^{77}Se$ coupling. It has been previously reported that $|^1J_{PSe}|$ coupling constants correlate linearly with the s-character of the phosphorus lone pair of electrons, which in turn is related to the electronegativity of the phosphorus substituents.[39,40] The $|^1J_{PSe}|$ coupling constants of **4**


dx.doi.org/10.1021/ic201309k | Inorg. Chem. 2012, 51, 2016−2030

**Scheme 2. Syntheses of Derivatives of 5-Diphenylphosphino-2,2′-bithiophene (5)**

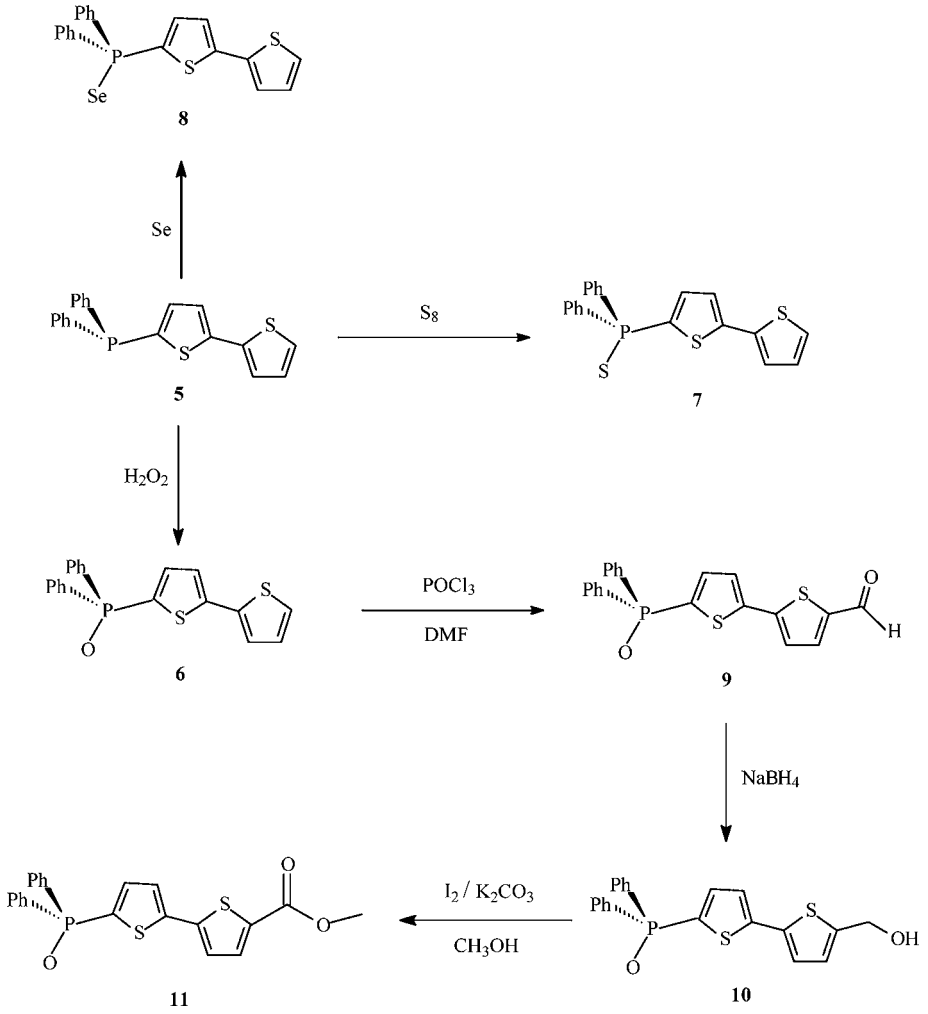


and **8** are consistent with trend because they are smaller than that of (2-furyl)$_3$PSe (793 Hz), which has more electron withdrawing 2-furyl groups, and larger than that of (*p*-MeOC$_6$H$_4$)$_3$PSe (708 Hz), which has more electron-donating *p*-MeOC$_6$H$_4$ groups.[41]

**Single Crystal X-ray Diffraction Analysis.** We have previously reported the crystal structures for the bithiophene derivatives, Ph$_2$(X)P(C$_4$H$_2$S)$_2$P(X)Ph$_2$ (X = O (**2**), S (**3**), and CH$_3^+$ I$^-$).[25] For each of the structures, the most interesting feature was the extensive $\pi-\pi$ stacking interactions that depended on the nature of the Ph$_2$(X)P group and the crystallization method. It is important to note that $\pi-\pi$ interactions lead not only to various solid state architectures but also may generate interesting electrical, optical and magnetic properties in the solid state.[42−44] Because it is of interest to investigate how the molecular conformation and unit cell packing type could be affected by varying the X group on the phosphorus, the number of Ph$_2$(X)P group, and the substitution on the bithiophene, the X-ray crystal structures of compounds **4**, **6**, **7**, and **10** have been determined. The molecular structures and the corresponding unit cell diagrams of **4**, **6**, **7**, and **10** are shown in Figures 1a and b, Figures 2a and b, Figures 3a and b, and Figures 4a and b, respectively. Intermolecular $\pi-\pi$ interactions and torsion angles are given in Table 2.

*X-ray Structure of* ***4****.* Compound **4**, which is symmetrically disubstituted with two Ph$_2$(Se)P groups, crystallizes with a center of symmetry at the midpoint of the bond bridging the two thienyl rings, and thus the two thienyl rings in **4** are coplanar and arranged in an anticonfiguration as is the case for **3** but not for either of the structures of **2**.[25] The P−Se bonds in **4** show two different rotations out of the plane of the adjacent thienyl rings as indicated by the S−C1−P−Se torsion angle of −35.2(2)° and the S′−C1′−P′−Se′ torsion angle of 129.4(2)°. These angles are quite similar to the S−C1−P−S torsion angles in **3** (36.6(3)° and −130.7(3)°).[25]

The similar molecular conformations of **3** and **4** result in similar packing of the molecules in the solid state with the bithiophenes of the two half molecules in the asymmetric unit oriented perpendicular to one another (Figure 1b). Offset-slipped $\pi-\pi$ stacking occurs between the phenyl rings on adjacent molecules, and point-to-face interactions occur both between the perpendicular thienyl rings and between the phenyl and thienyl rings of adjacent molecules (Table 2).

*X-ray Structure of* ***6****.* Unlike the disubstituted phosphine oxide, **2**, the monosubstituted analogue, **6**, cannot crystallize on a center of symmetry. The two thienyl rings in **6** are twisted relative to one another with the dihedral angle between the mean planes through the two thienyl rings being 15.2°.The P−O bond is nearly in the plane of the adjacent


dx.doi.org/10.1021/ic201309k | *Inorg. Chem.* 2012, 51, 2016−2030

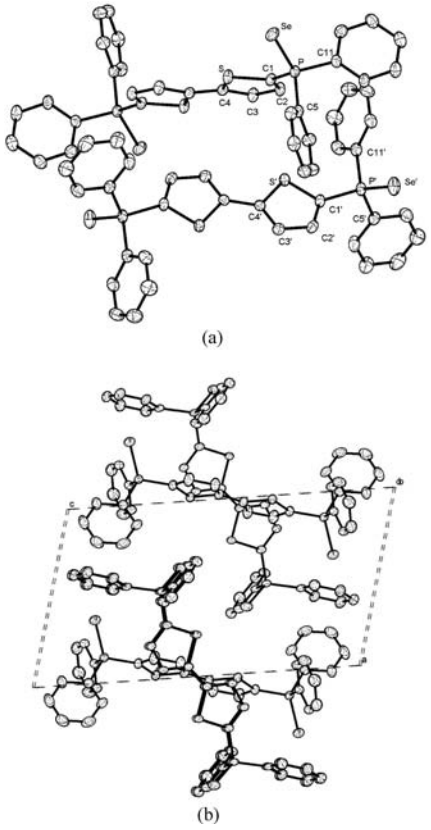

**Figure 1.** (a) Molecular structure of **4**. Hydrogen atoms are omitted and the atomic displacement ellipsoids are drawn at 25% probability. (b) The *ac* face of the unit cell of **4**. Hydrogen atoms are omitted and thermal ellipsoids are shown at 15% probability.

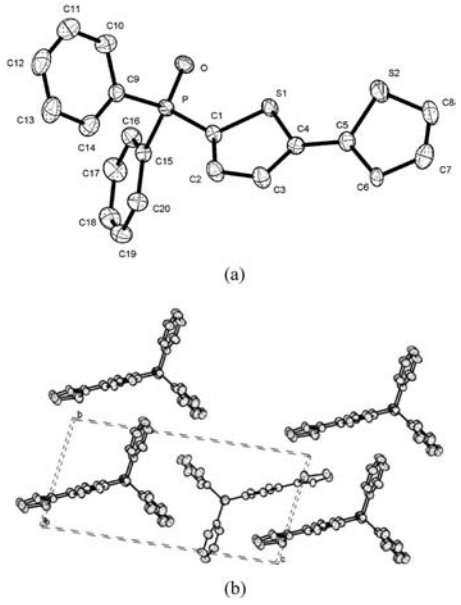

**Figure 2.** (a) Molecular structure of **6**. Hydrogen atoms are omitted and the atomic displacement ellipsoids are drawn at 25% probability. (b) The *bc* face of the unit cell of **6**. Hydrogen atoms are omitted and thermal ellipsoids are shown at 15% probability.

thienyl ring as indicated by the C2−C1−P−O torsion angle of 174.6(3)°.

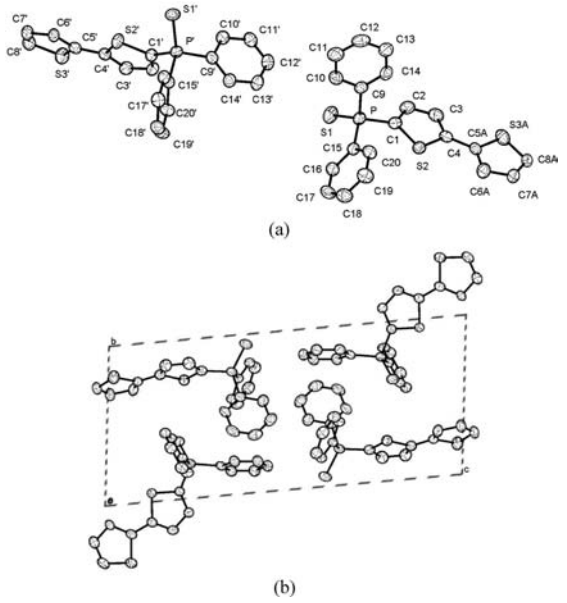

**Figure 3.** (a) Molecular structure of **7**. Hydrogen atoms are omitted and the atomic displacement ellipsoids are drawn at 25% probability. (b) The *bc* face of the unit cell of **7**. Hydrogen atoms are omitted and thermal ellipsoids are shown at 15% probability.

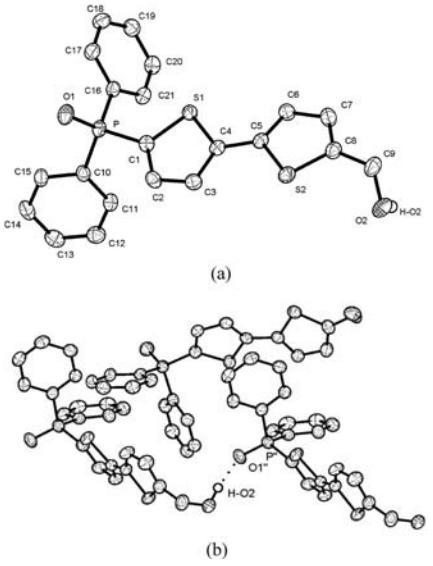

**Figure 4.** (a) Molecular structure of **10**. Hydrogen atoms are omitted and the atomic displacement ellipsoids are drawn at 25% probability. (b) Packing diagram of **10** showing hydrogen bonding. Hydrogen atoms are omitted and thermal ellipsoids are shown at 15% probability.

Both offset-slipped and point-to-face $\pi-\pi$ stacking interactions are observed in **6** (Figure 2b). The offset-slipped interactions occur both between the thienyl rings on adjacent molecules and between the phenyl rings. The point-to-face interactions occur both between the perpendicular phenyl rings and between the perpendicular thienyl and phenyl rings. These interactions allow all of the bithiophene groups in the crystal to have similar orientations, and the least-squares planes through all of the bithiophenes in the crystal to be parallel.


dx.doi.org/10.1021/ic201309k | *Inorg. Chem.* 2012, 51, 2016−2030

**Table 2. Intermolecular $\pi-\pi$ Interactions and Torsion Angles in the Crystal Structures of 4, 6, 7, and 10**

| crystal | offset-slipped | interplanar distance (Å) | point-to-face | atom-centroid distance (Å) | torsion angles (deg) | |
|---|---|---|---|---|---|---|
| **4** | phenyl−phenyl[a] | 3.776 | thienyl−thienyl[b] | 3.691 | S−C1−P−Se | −35.2(2) |
| | | | phenyl−thienyl[b] | 3.758 | S′−C1′−P′−Se′ | 129.4(2) |
| **6** | thienyl−thienyl[a] | 3.681 | phenyl−phenyl[b] | 3.665 | C2−C1−P−O | 174.6(3) |
| | phenyl−phenyl[a] | 4.058 | thienyl−phenyl[b] | 3.736 | | |
| **7** | | | phenyl−phenyl[b] | 3.690 | C2−C1−P−S1 | 45.5(3) |
| | | | | | C2′−C1′−P′−S1′ | 147.3(3) |
| **10** | | | | | C2−C1−P−O1 | 74.9(3) |

[a]The offset-slipped $\pi-\pi$ interactions occur between the two parallel but displaced rings on adjacent molecules. [b]The point-to-face $\pi-\pi$ interactions occur between the two perpendicular rings on adjacent molecules.

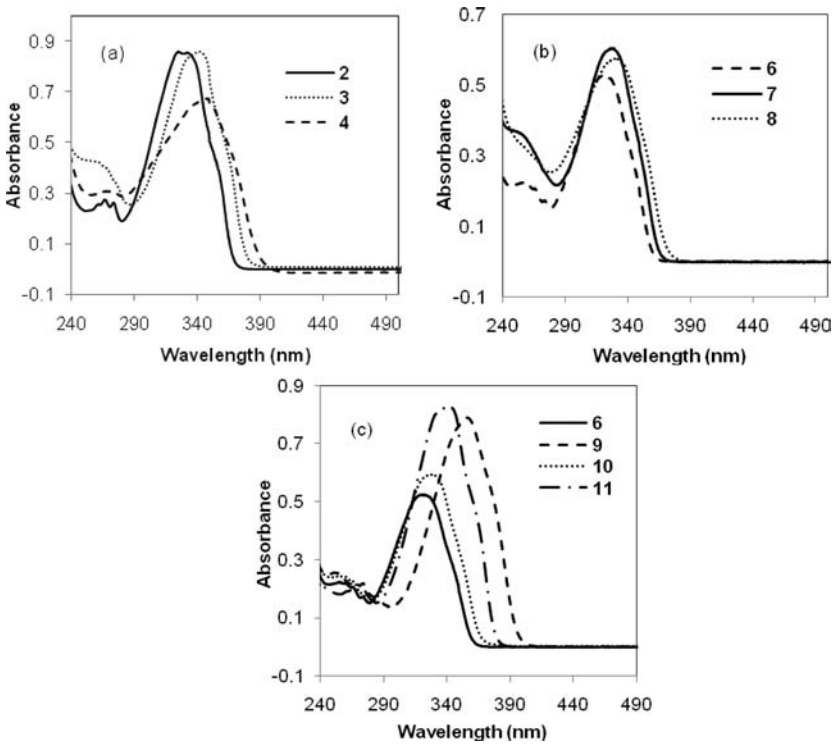


**Figure 5.** UV−vis absorption spectra of $3.0 \times 10^{-4}$ mol/L chloroform solutions of bithiophene derivatives of (a) **2**−**4**; (b) **6**−**8**; and (c) **6**, **9**, **10** and **11** in a 1-mm cell.

*X-ray Structure of 7.* In spite of the very similar chemical structures of **6** and **7**, the molecular conformations and packing of these two molecules are quite different. In compound **7**, the two thienyl rings are nearly coplanar (dihedral angle 7.0°). Unlike the P−O bonds in **6**, which are nearly in the plane of the bithiophene, the P−S bonds in **7** are rotated out of the plane of the adjacent thienyl ring as indicated by the C2−C1−P−S1 torsion angle of 45.5(3)° and the C(2′)−C(1′)−P′−S(1′) torsion angle of 147.3(3)°.

In contrast to **6**, only point-to-face $\pi-\pi$ stacking interactions are observed between the perpendicular phenyl rings on adjacent molecules in **7** (Figure 3b). This results in the bithiophenes having two different orientations with the least-squares planes through the bithiophenes in one of the molecule nearly perpendicular to the least-squares planes through the bithiophenes in the other molecule.

*X-ray Structure of 10.* Compound **10** does not have a center of symmetry, and the thiophene rings are not coplanar (dihedral angle of 12.8°). The P−O bonds are rotated out of the plane of the adjacent thienyl ring, as indicated by the C2−C1−P−O1 torsion angle of 74.9(3)°.

The introduction of a hydroxymethyl group at the 5′-position of **6** results in a very different solid state structure of **10** in which no $\pi-\pi$ interactions between the thienyl and phenyl rings are observed. Instead, an intermolecular hydrogen bonding interaction between the hydroxyl hydrogen on one molecule and the phosphoryl oxygen on the other is observed. This seems to be relatively strong based on the O2 to O1″ distance of 2.744(3) Å and the H−O2 to O1″ distance of 1.79(5) Å.

**Electronic Absorption Spectra.** Figure 5 shows the linear absorption spectra of $3.0 \times 10^{-4}$ M solutions of **2**−**4** and **6**−**11** in chloroform. The absorption band maxima and the molar absorptivities are given in Table 3. Each compound exhibits a broad absorption band between 300 and 400 nm. Regardless of the number and type of phosphine substitution and the nature of the 5′-substituent, these compounds are essentially transparent above 430 nm, providing a broad optical window in the violet to blue region in which optical power limiting may occur.


dx.doi.org/10.1021/ic201309k | *Inorg. Chem.* 2012, 51, 2016−2030

**Table 3. Emission Data for Compounds 2−11 in Chloroform Solution**

| compound | $\lambda_{abs}$/nm ($\varepsilon$/dm$^3$·mol$^{-1}$·cm$^{-1}$)[a] | $\lambda_{em}$/nm[b] | $\Delta\lambda$[c] (nm) | $\Phi$[d] |
|---|---|---|---|---|
| $T_2$[e] | 315 (1.24 × 10$^4$) | 369 | 54 | 0.012 |
| **2** | 326 (2.86 × 10$^4$) | 390 | 64 | 0.17 |
| **3** | 342 (2.86 × 10$^4$) | 400 | 58 | 0.0056 |
| **6** | 321 (1.75 × 10$^4$) | 384 | 63 | 0.15 |
| **7** | 328 (2.01 × 10$^4$) | 387 | 59 | 0.0052 |
| **8** | 329 (1.92 × 10$^4$) | 385 | 56 | 0.0037 |
| **9** | 356 (2.63 × 10$^4$) | 424 | 68 | 0.014 |
| **10** | 329 (1.98 × 10$^4$) | 393 | 64 | 0.26 |
| **11** | 340 (2.77 × 10$^4$) | 400 | 60 | 0.17 |

[a]Linear absorption band maximum and molar absorptivity in $CHCl_3$ solution. [b]Emission band maximum in $CHCl_3$ solution. [c]Stokes shift. [d]Emission quantum yield using quinine sulfate solution in 0.1 M $H_2SO_4$ as the reference. [e]Bithiophene.

The linear absorption maxima of these compounds are blue-shifted relative to those of the corresponding terthiophenes,[24] and those for the disubstituted bithiophenes are at longer wavelengths than are those for the monosubstituted bithiophenes with the same X groups. The linear absorption maxima for the disubstituted bithiophenes are slightly red-shifted as the atomic number of X increases (**2** (X = O), $\lambda_{abs}$ = 326 nm; **3** (X = S), $\lambda_{abs}$ = 342 nm; **4** (X = Se), $\lambda_{abs}$ = 348 nm). In contrast, changing the X group has a smaller effect on the linear absorption maxima of the monosubstituted bithiophenes (**6** (X = O), $\lambda_{abs}$ = 321 nm; **7** (X = S), $\lambda_{abs}$ = 328 nm; **8** (X = Se), $\lambda_{abs}$ = 329 nm). This means that the difference between the maximum wavelengths for the absorption maxima of the disubstituted and monosubstituted bithiophenes also increases as the atomic number of X increases. This result is in agreement with our density functional theory (DFT) calculations that show smaller HOMO−LUMO energy differences for the disubstituted bithiophenes than for their monosubstituted analogues (see Supporting Information).

As expected, the linear absorption maxima of the monosubstituted bithiophenes are very sensitive to the nature of the R substituent at the 5′-position, and a red shift of the linear absorption maximum is observed as a more highly conjugated group is introduced at this position (**6** (R = H): $\lambda_{abs}$ = 321 nm; **10** (R = $CH_2OH$): $\lambda_{abs}$ = 329 nm; **11** (R = $CO_2Me$): $\lambda_{abs}$ = 340 nm; **9** (R = CHO): $\lambda_{abs}$ = 356 nm). This redshift is consistent with our DFT calculations that the HOMO−LUMO energy difference for the monosubstituted bithiophenes decreases in the order **6** > **10** > **11** > **9** (see Supporting Information). The substituent at the 5′-position also affects the molar absorptivity. In more conjugated compounds the molar absorptivity increases in the order **6** ≈ **10** < **11** ≈ **9**.

**Emission Spectra.** Our previous study of the solution phase fluorescence spectra of $Ph_2(X)P$-substituted terthiophenes demonstrated that both the emission maxima and fluorescence quantum yields could be tuned by varying the number of $Ph_2(X)P$ groups, the X group and the 5″-substituent on the terthiophene.[24] To determine how replacing a terthiophene with a bithiophene could affect the fluorescence properties, the emission spectra of compounds **2**−**4** and **6**−**11** have been measured. The normalized emission spectra are shown in Figure 6. The quantum yields for these compounds have been determined using quinine sulfate solution in 0.1 M $H_2SO_4$ as the reference and are summarized in Table 3. All the compounds exhibit maximum emission bands between 380 and 430 nm, and these maxima are blue-shifted relative to those of their terthiophene analogues (which have emission band maxima between 430 and 480 nm).[24]

The number of $Ph_2(X)P$ groups attached to the bithiophene has only a slight effect on either the emission wavelengths or the quantum yields. In contrast, the nature of the X substituent of the $Ph_2(X)P$ group has a significant effect on the emission quantum yields of both the disubstituted and monosubstituted bithiophenes but has only a small effect on the emission wavelengths. For the disubstituted bithiophenes, the quantum yield of **2** is significantly higher than that of **3**, and no fluorescence is observed for **4**. The trend in quantum yields for the monosubstituted bithiophenes is quite similar with **6** exhibiting a significantly higher quantum yield than either **7** or **8**. The lack of fluorescence for **4**, and the much weaker fluorescence for **8**, both of which contain Se as the X substituent, may be due to the heavy-atom effect in which spin and orbital interactions increase the probability for intersystem crossing to the triplet state and decrease the fluorescence.[45]

The nature of the organic (R) substituent in the monosubstituted bithiophenes also has a significant effect on both the emission wavelength and emission quantum yields. As is the case for the electronic absorption spectra, a red shift of the emission maximum is observed as the R substituent is varied in the order **6** (R = H), **10** (R = $CH_2OH$), **11** (R = $CO_2Me$), **9** (R = CHO) consistent with the increasing conjugation of the organic substitutent. The effects of the organic substituents on the quantum yields are more complex, and DFT calculations, discussed in the next section, have been carried out to gain insight into these structure−property relationships.

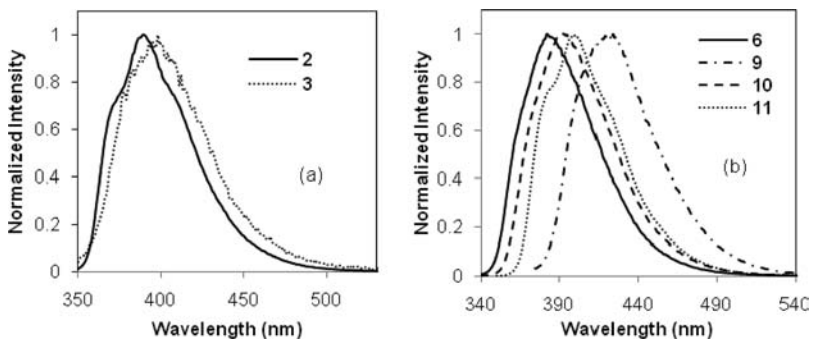


**Figure 6.** Normalized emission spectra of 3.0 × 10$^{-6}$ M chloroform solutions of (a) **2**−**3**, (b) **6**, and **9**−**11** in a 10-mm cell.


dx.doi.org/10.1021/ic201309k | Inorg. Chem. 2012, 51, 2016−2030

The effects of variations in the substituents of the $Ph_2(O)P$-substituted bithiophenes on the quantum yields are quite different from those previously reported for $Ph_2(O)P$-substituted terthiophenes as shown in Table 4.[24] Adding one $Ph_2(O)P$ group to terthiophene to form $Ph_2(O)P(C_4H_2S)_3H$ has little effect on the quantum yield, while adding a second $Ph_2(O)P$ group to form $Ph_2(O)P(C_4H_2S)_3P(O)Ph_2$ increases the quantum yield by a factor of 2.7 times relative to that of terthiophene.[24] In contrast, adding one $Ph_2(O)P$ group to bithiophene to form $Ph_2(O)P(C_4H_2S)_2H$ (**6**) increases the quantum yield by a factor of 13 relative to that of bithiophene while adding a second $Ph_2(O)P$ group to form $Ph_2(O)P(C_4H_2S)_2P(O)Ph_2$ (**2**) causes only a slight increase in the quantum yield. The net result is that the quantum yields of $Ph_2(O)P(C_4H_2S)_3P(O)Ph_2$ and **2** are essentially the same.

**Table 4. Comparison of the Emission Data of the Bithiophene Derivatives and Those of Analogous Terthiophene Derivatives**

| | $n = 3$ | | $n = 2$ | | |
|---|---|---|---|---|---|
| compound | $\Phi_1$[a] | $\Phi_1/\Phi_{T3}$[b] | $\Phi_2$[c] | $\Phi_2/\Phi_{T2}$[d] | $\Phi_2/\Phi_1$[e] |
| $H(C_4H_2S)_nH$ | 0.059[f] | 1.0 | 0.012 | 1.0 | 0.20 |
| $Ph_2(O)P(C_4H_2S)_nH$ | 0.055 | 0.94 | 0.15 | 13 | 2.7 |
| $Ph_2(O)P(C_4H_2S)_nP(O)Ph_2$ | 0.16 | 2.7 | 0.17 | 14 | 1.1 |
| $Ph_2(O)P(C_4H_2S)_nCO_2Me$ | 0.077 | 1.3 | 0.17 | 14 | 2.2 |
| $Ph_2(O)P(C_4H_2S)_nCH_2OH$ | 0.089 | 1.5 | 0.26 | 22 | 2.9 |

[a]Quantum yields of the terthiophene derivatives in $CH_2Cl_2$ solutions using terthiophene as the reference. [b]The ratio of the quantum yield relative to terthiophene. [c]Quantum yields of the bithiophene derivatives in $CHCl_3$ solutions using quinine sulfate solution in 0.1 M $H_2SO_4$ as the reference. [d]The ratio of the quantum yield relative to bithiophene. [e]The ratio of the quantum yield between the bithiophenes derivatives and the terthiophene analogues with the same substituent. [f]Data is from ref 46 and is for a $CH_2Cl_2$ solution of terthiophene.

The most significant difference between the bithiophene and terthiophene derivatives is that adding one $Ph_2(O)P$ and one organic substituent to bithiophene causes a much greater increase in the quantum yield than does adding the same groups to terthiophene. The quantum yields of $Ph_2(O)P(C_4H_2S)_2H$ (**6**), $Ph_2(O)P(C_4H_2S)_2P(O)Ph_2$ (**2**), $Ph_2(O)P(C_4H_2S)_2CO_2Me$ (**11**) and $Ph_2(O)P(C_4H_2S)_2CH_2OH$ (**10**) are significantly larger than that of bithiophene (factors of 13, 14, 14, and 22 respectively), whereas similar substitutions in terthiophenes only cause a modest increase in the quantum yields over that of terthiophene (factors of 0.94, 2.7, 1.3, and 1.5 respectively). The differences in the increases are such that the substituted bithiophenes generally have larger quantum yields than do the terthiophenes with the same substituents even though the quantum yield of terthiophene is five times larger than that of bithiophene. For example, the quantum yield of $Ph_2(O)P(C_4H_2S)_2CH_2OH$ (**10**) is 2.9 times higher than that of the terthiophene analogue, $Ph_2(O)P(C_4H_2S)_3CH_2OH$.

**Theoretical Study of Fluorescent Properties for Bithiophene Derivatives.** Insight into the different effects of organic substituents on the fluorescent properties of the $Ph_2(X)P$-substituted bithiophenes and terthiophenes may be provided by DFT calculations. For example, Stott and Wolf have reported that DFT calculations on the ground and first excited singlet states of the parent phosphines of the two classes, $Ph_2P(C_4H_2S)_nPPh_2$ (n = 2 (**1**), 3) demonstrate that the phosphorus group contributes more to the HOMO and LUMO in the bithiophene than in the terthiophenes.[27] Further, a recent study of oligoarylfluorenes has shown that many important molecular photophysical parameters can be directly calculated by the time-dependent density functional theory (TDDFT) and the calculated lifetimes are in good agreement with experimental data.[36,37]

*(a) Frontier Molecular Orbitals.* To gain qualitative insight into how the various substituents of the $Ph_2(X)P$-substituted bithiophenes affect excitation and fluorescence, the frontier orbitals (ground state HOMOs and LUMOs at the B3LYP/6-31G(d)// B3LYP/6-31G(d) level of theory) of **2**–**3**, **6**–**7**, and **9**–**11** are shown in Figure 7.

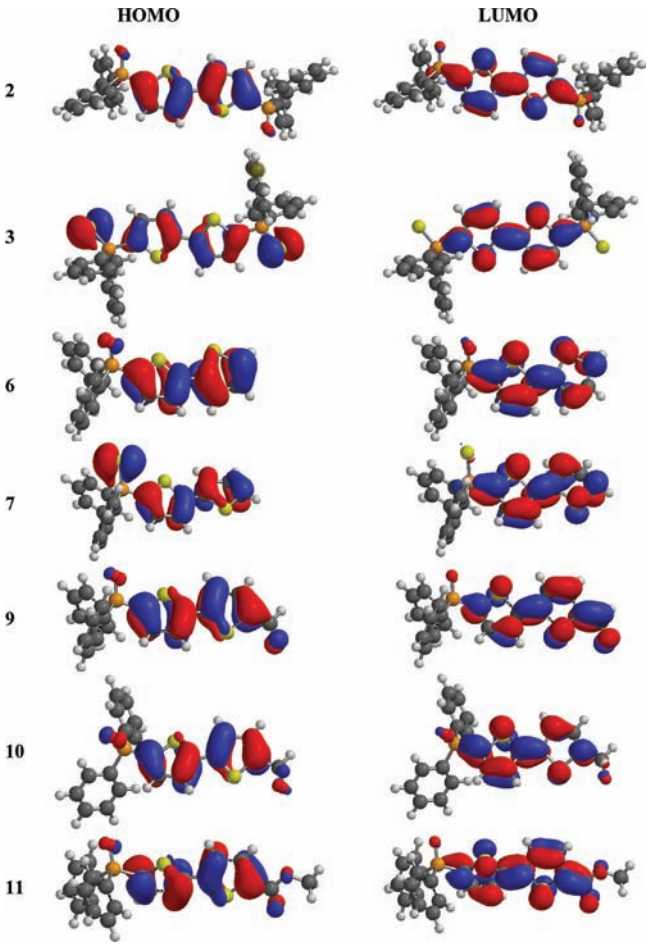


**Figure 7.** Frontier molecular orbitals for compounds **2**–**3**, **6**–**7**, and **9**–**11** calculated by the B3LYP/6-31G* method.

As shown in Figure 7, the HOMO of **3** has significant contribution from the two P–S bonds by bonding interaction with the bithienyl $\pi$-system, whereas the LUMO is mainly localized on the bithienyl group. In contrast, the HOMO of **2** exhibits a moderate O lone-pair character. Similarly the HOMO of **7** exhibits a significant P–S bond character while the HOMO of **6** shows just a moderate O lone-pair character. According to a simple picture of oscillator strength being roughly proportional to spatial extent of the HOMO and LUMO, the oscillator strength of **3** and **7** are expected to be smaller, i.e. for X = S rather than X = O.

Both the HOMOs and the LUMOs of the $Ph_2(O)P$-substituted bithiophenes **6** and **9**–**11** have large contributions from the


dx.doi.org/10.1021/ic201309k | Inorg. Chem. 2012, 51, 2016–2030

Table 5. Theoretical Study of Emission Spectra by TD-B3LYP/6-31G(d) Method at CIS/6-31G(d) Optimized Geometry

| | calculated | | | | | estimated | | experimental | | |
|---|---|---|---|---|---|---|---|---|---|---|
| compound | $E_{flu}$[a] (eV) | $\lambda_{em}$ (nm)/ error (%)[b] | $f$[c] | $\tau_n$[d] (ns) | $k_f$[e] ($10^9$/s) | $\tau_s$[f] (ns) | $k_{nr}$[g] ($10^9$/s) | $\lambda_{em}$ (nm) | $\tau_s$ (ns) | $\Phi$ |
| $T_2$ | 3.57 | 347/−5.9 | 0.44 | 4.11 | 0.243 | 0.049 | 20.0 | 369 | 0.051[h] | 0.012 |
| $T_3$ | 2.95 | 420/−2.3 | 0.84 | 3.15 | 0.317 | 0.19 | 5.06 | 430 | 0.18[h] | 0.059 |
| **2** | 3.26 | 380/−2.5 | 0.98 | 2.21 | 0.452 | 0.38 | 2.21 | 390 | | 0.17 |
| **3** | 2.88 | 431/7.7 | 0.31 | 8.88 | 0.113 | 0.050 | 20.1 | 400 | | 0.0056 |
| **6** | 3.41 | 364/−5.2 | 0.67 | 2.95 | 0.339 | 0.44 | 1.92 | 384 | | 0.15 |
| **7** | 3.11 | 398/2.8 | 0.21 | 11.06 | 0.0904 | 0.058 | 17.3 | 387 | | 0.0052 |
| **9** | 3.17 | 391/−7.7 | 0.84 | 2.72 | 0.368 | 0.038 | 25.9 | 424 | | 0.014 |
| **10** | 3.33 | 373/−5.1 | 0.76 | 2.74 | 0.365 | 0.71 | 1.04 | 393 | | 0.26 |
| **11** | 3.16 | 392/−2.0 | 0.80 | 2.89 | 0.346 | 0.49 | 1.69 | 400 | | 0.17 |

[a]Fluorescence energy. [b]Error = $(\lambda_{em}^{calcd} - \lambda_{em}^{exptl})/\lambda_{em}^{exptl}$. [c]Oscillator strength. [d]Intrinsic natural fluorescence lifetime. [e]Fluorescence rate constant $k_f = \tau_n^{-1}$. [f]Excited state lifetime $\tau_s = \tau_n\Phi$ . [g]Nonradiative rate constant $k_{nr} = k_{isc} + k_{ic} + k_{ec}$. [h]$\tau_s$ values for $T_2$ and $T_3$ are from reference[46] and converted to chloroform solution.

5′ organic substituents: the carbonyl oxygen in the formyl group in **9**, the hydroxyl oxygen in the hydroxymethyl group in **10**, and the carbonyl oxygen and ester oxygen in the methyl ester group in **11**. The largest interaction is between the thiophene ring and the carbonyls in **9** and **11**, with a nonbonding $\pi$-interaction at the carbonyl carbon in the HOMOs, and a carbonyl $\pi^*$ in the LUMOs. The delocalization of the HOMO and LUMO in **9** and **11** is expected to lower the HOMO−LUMO gap and hence give longer transition wavelengths.

*(b) Emission Spectra.* For applications in OLEDs and in sensor protection, the excited state lifetimes of the compounds in this study are important parameters. The fluorescence energies, maximum emission wavelengths and oscillator strengths of the compounds in this study have been calculated using the same TDDFT computational methods and are listed in Table 5. The intrinsic natural fluorescence lifetimes for spontaneous emission, $\tau_n$, were then calculated from these parameters using the Einstein transition probabilities according to eq 2[36,47]

$$\tau_n = \frac{c^3}{2(E_{flu})^2 f} \quad (2)$$

where $c$ is the velocity of light, $E_{flu}$ is the fluorescence energy, and $f$ is the oscillator strength.

The calculated maximum emission wavelengths in Table 5 are in good agreement with experimental data, with errors in calculated maximum emission wavelengths relative to the experimental emission wavelengths ranging from −7.7% to 7.7%. Except that the calculations for the sulfur containing **3** and **7** overestimate the wavelengths, all other calculated fluorescence wavelengths are slightly shorter than experiment. These errors are comparable to those found for oligoarylfluorene derivatives.[36,37]

The excited state lifetime, $\tau_s$, was estimated from the calculated intrinsic natural lifetime, $\tau_n$, and the experimental quantum yield, $\Phi$, and using the equation of $\tau_s = \tau_n\Phi$. The lifetime, $\tau_s$, will only be accurate if the computation method is able to accurately calculate the $\tau_n$. Comparisons of estimated and experimental lifetimes for closely related compounds suggest that this is the case. The estimated excited state lifetimes for both $T_2$ and $T_3$ differ from the experimental excited state lifetimes by 3.9% and 5.5%, respectively as shown in Table 5. Estimated excited state lifetimes of oligoarylfluorene derivatives, which are closely related to the compounds **2**−**3**, **6**−**7**, and **9**−**11** in this study, are also quite similar to the experimental values.[36,37]

Both the fluorescence rate constant, $k_f$, which is the reciprocal of intrinsic lifetime, $\tau_n$, and nonradiative rate constant, $k_{nr}$, which is defined as $k_{nr} = k_{isc} + k_{ic} + k_{ec}$ where $k_{isc}$ is intersystem crossing rate constant, $k_{ic}$ and $k_{ec}$ are the respective rate constants for internal and external conversion decay, affect the fluorescence quantum yield, $\Phi$, as shown by eq 3[45,46]

$$\Phi = \frac{k_f}{k_f + k_{nr}} \quad (3)$$

Because both $\Phi$ (Table 4) and $k_f$ (Table 5) are available for each of the $Ph_2(X)P$-substituted bithiophenes in this study, eq 3 can be used to determine $k_{nr}$.

From the data in Table 5, it is quite clear that changes in the number of $Ph_2(X)P$ groups and the nature of the X substituent in the $Ph_2(X)P$-substituted bithiophenes affect both $k_f$ and $k_{nr}$ values. The higher $\Phi$ values of **2** and **6** relative to those of **3** and **7** and $T_2$ are because of combination of larger $k_f$ values and the smaller $k_{nr}$ values for **2** and **6**. By comparison with $T_2$, **2** and **6** have 10-fold smaller $k_{nr}$ values than $T_2$, whereas **3** and **7** have approximately the same large $k_{nr}$ values as $T_2$. On the other hand, the O substituent in **2** and **6** results in larger $k_f$ values while the S substituent in **3** and **7** makes $k_f$ values smaller relative to $T_2$. The larger $k_f$ values for **2** and **6** are consistent with the greater overlaps between the LUMO and the HOMO in **2** and **6** shown in Figure 7.

Contrary to the effects of the $Ph_2(X)P$ groups, the organic substituents in the $Ph_2(O)P$-substituted bithiophenes **6** and **9**−**11** primarily affect the $k_{nr}$ values. All four compounds have $k_f$ values that differ by no more than 10% suggesting that the organic substituent has little effect on the $k_f$ values. In contrast, the $k_{nr}$ value of **9** (R = CHO) is larger than those of **6** (R = H), **10** (R = $CH_2OH$) and **11** (R = $CO_2Me$) by an order of magnitude, suggesting that the primary effect of the organic substituent is to alter the nonradiative decay pathways. The large $k_{nr}$ value for **9** is presumably due to the deactivation of an excited electronic state resulting from interaction and energy transfer between the excited molecule and the solvent or other solutes.[48]

**Nonlinear Optical Characterization.** To optimize optical limiting performance in a class of materials, it is necessary to maximize the nonlinear optical absorption (or reverse saturable absorption) of those materials, which is both wavelength


dx.doi.org/10.1021/ic201309k | Inorg. Chem. 2012, 51, 2016−2030

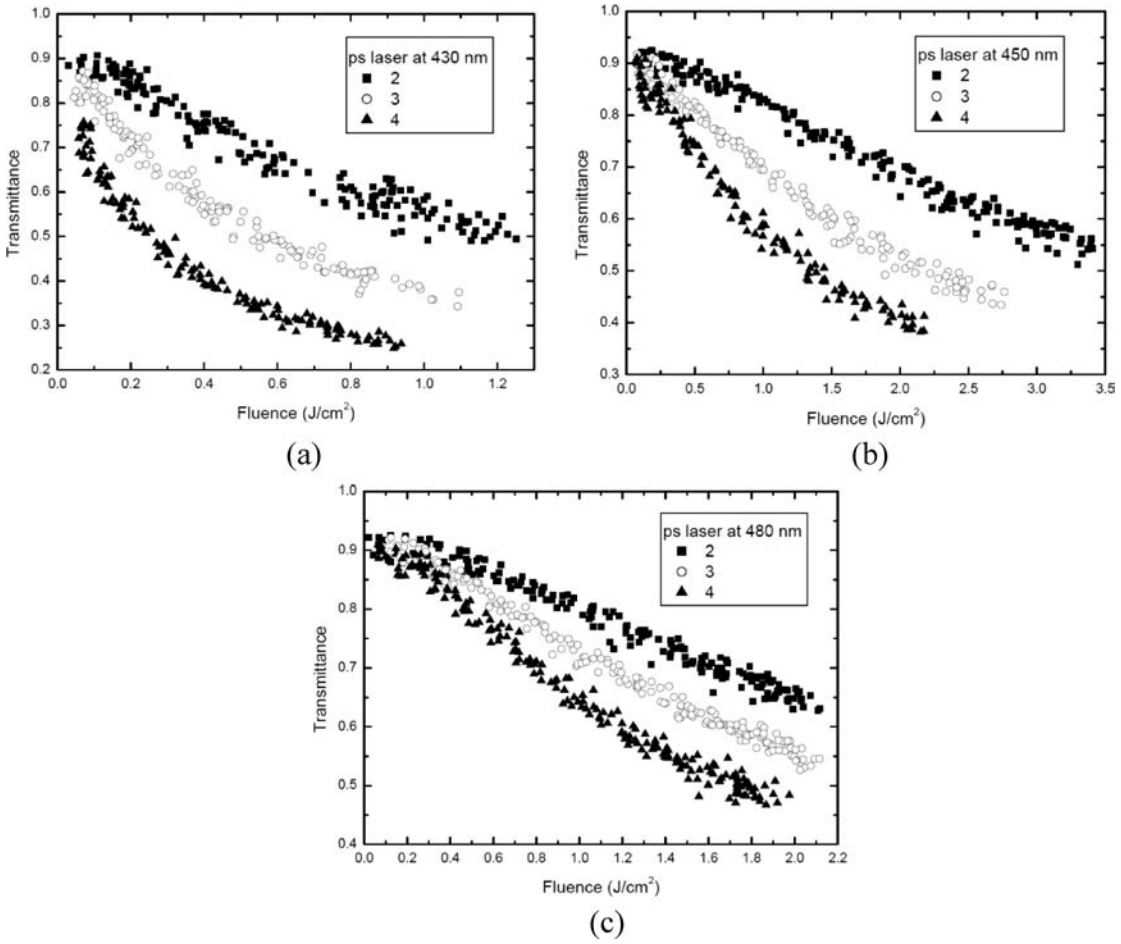


**Figure 8.** Comparison of the nonlinear transmittances of $CH_2Cl_2$ solutions of **2**−**4** at the same concentration of 0.067 M with 27 ps laser pulses at (a) 430, (b) 450, and (c) 480 nm. The NLO absorption for **4** shows stronger than that for **2** and **3** at the same concentration and the same wavelength.

and concentration dependent.[49] Our preliminary study of two $Ph_2(X)P$-substituted bithiophenes demonstrated that the NLO absorption of a saturated $CH_2Cl_2$ solution of $Ph_2(S)P(C_4H_2S)_2P(S)Ph_2$ (**3**) was stronger than that of a saturated $CH_2Cl_2$ solution of $Ph_2(O)P(C_4H_2S)_2P(O)Ph_2$ (**2**) at wavelengths of 420, 430, and 440 nm for 27 ps laser pulses.[26] This suggests that the nonlinear absorption is very sensitive to the chalcogen attached to the nonbonding pair of electrons on the diphenylphosphino group, and thus that the violet-blue NLO absorbers could be further improved by attaching an even heavier chalcogen to the $Ph_2P$ substituent.

To test this possibility, $Ph_2(Se)P(C_4H_2S)_2P(Se)Ph_2$ (**4**) was synthesized. To compare the NLO transmittances of **2**, **3**, and **4** on a per molecule basis, the NLO transmittances of 0.067 mol/L $CH_2Cl_2$ solutions of the compounds were measured at 430, 450, and 480 nm (Figure 8). At 430 nm, when the incident fluence reaches 0.9 J/cm$^2$, the transmittance drops to 60% for **2**, 41% for **3**, and 25% for **4**. The threshold for NLO absorption, defined as the incident fluence at which the transmittance falls to 50%, is 1.2 J/cm$^2$ for **2**, 0.55 J/cm$^2$ for **3**, and 0.27 J/cm$^2$ for **4**. These results demonstrate that the NLO absorption increases with the increasing of atomic weight of X (Se > S > O). The same trend is seen at 450 and 480 nm, but all of the chromophores show a decrease in nonlinear absorption at these wavelengths.

The fact that saturated solutions of the bithiophene derivatives can be used without suffering from high linear transmission losses means that increasing the solubility of the molecules could also give a stronger NLO absorption. A limitation of the bithiophenes that are symmetrically disubstituted with two $Ph_2(X)P$ groups (X = O (**2**), S (**3**), Se (**4**)) is that they all have relatively low solubilities (Table 5). In light of this, the analogous bithiophenes substituted with a single $Ph_2(X)P$ group (X = O (**6**), S (**7**), Se (**8**)) were prepared. As shown by the data in Table 6, the bithiophenes with a single $Ph_2(X)P$ group are approximately ten times more soluble than are those with two $Ph_2(X)P$ groups. Saturated

**Table 6. Saturation Concentration of $Ph_2(X)P$-Substituted Bithiophene Derivatives 2−10**

| compound | saturation conc. (mol/L)/solvent |
|---|---|
| **2** | 0.184/$CH_2Cl_2$ |
| **3** | 0.217/$CH_2Cl_2$ |
| **4** | 0.103/$CH_2Cl_2$ |
| **6** | 2.11/$CHCl_3$ |
| **7** | 2.66/$CHCl_3$ |
| **8** | 1.66/$CHCl_3$ |
| **9** | 0.851/$CHCl_3$ |
| **10** | 0.909/$CHCl_3$ |


dx.doi.org/10.1021/ic201309k | Inorg. Chem. 2012, 51, 2016−2030

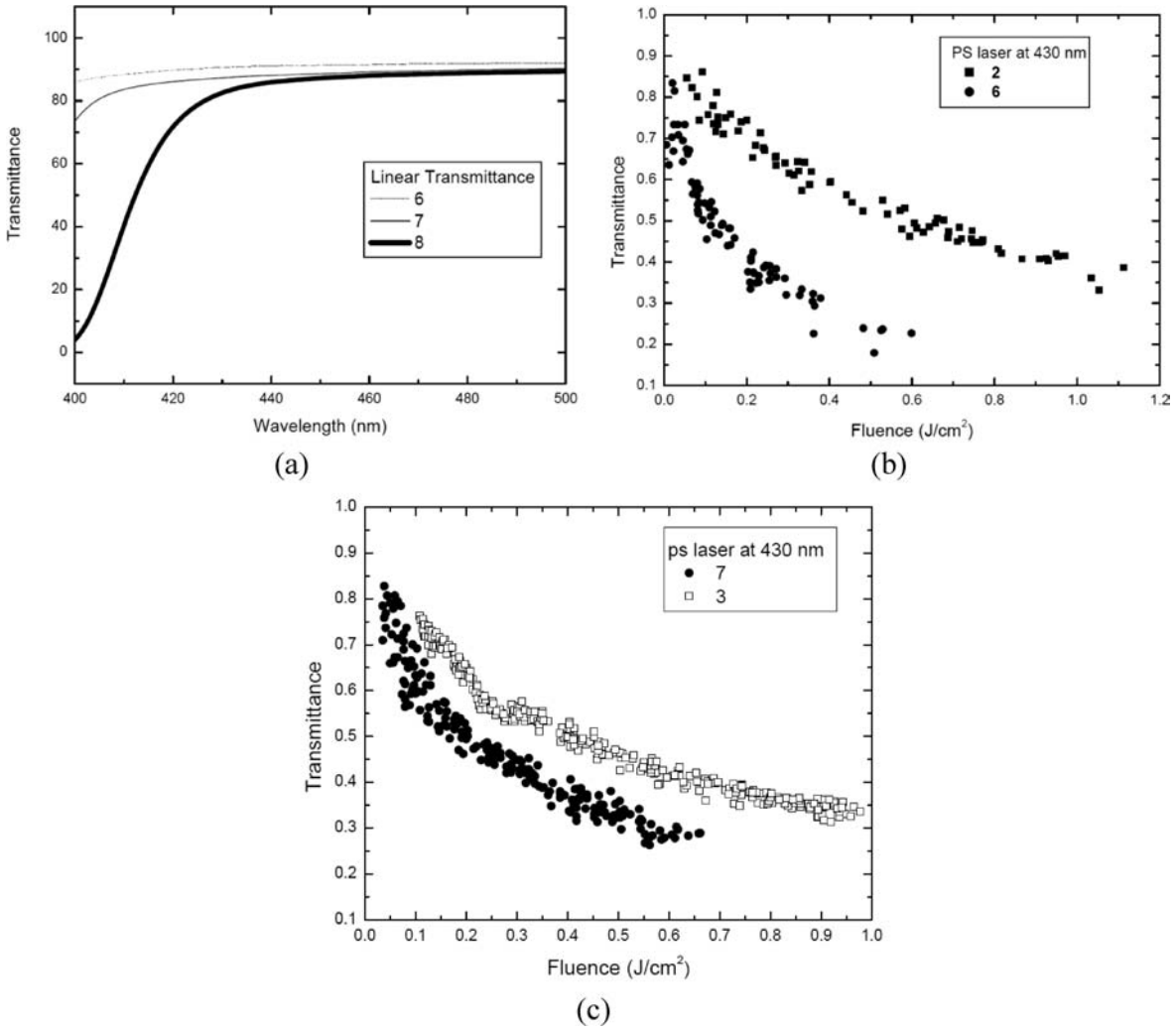


**Figure 9.** (a) Linear transmittances of saturated $CHCl_3$ solutions of **6**–**8** with all solutions having linear transmittances greater than 80% from 430 to 500 nm. Comparison of the nonlinear transmittances of (b) saturated solutions for **2** and **6** and (c) saturated solutions for **3** and **7**, with 27 ps laser pulses at 430 nm.

solutions of these compounds are still sufficiently transparent in the violet and blue regions of the visible spectrum that they have linear transmittances above 80% from 430 to 500 nm (Figure 9a).

The high linear transmittances of saturated solutions of bithiophenes substituted with a single $Ph_2(X)P$ group allow the nonlinear absorptions of these solutions to be evaluated at all wavelengths in the violet and blue regions. As shown in Figure 9b and c, the nonlinear absorption of the saturated solution for the asymmetric compound **6** is significantly larger than that of the symmetric compound **2** at 430 nm. A comparison of the nonlinear absorption of the saturated solution for **7** and **3** shows a similar trend with **7** exhibiting much stronger nonlinear absorption than **3** at 430 nm. When the incident fluence reaches 0.6 J/cm$^2$, the transmittance drops to 49% for **2**, 42% for **3**, 23% for **6**, and 30% for **7**. The optical limiting threshold when the transmittance falls to 50% is 0.60 J/cm$^2$ for **2**, 0.40 J/cm$^2$ for **3**, 0.10 J/cm$^2$ for **6**, and 0.18 J/cm$^2$ for **7**. The saturated chloroform solutions of the **6** and **7**, exhibit the best NLO absorption of picosecond laser pulses that has been reported.

To eliminate the effect of solution concentrations and allow comparison of the NLO absorbances of the monosubstituted bithiophenes to be made on a per molecule basis, the NLO transmittances of 1.66 mol/L $CHCl_3$ solutions of **6**, **7**, and **8** were measured at 430, 450, and 480 nm. As shown in Figures 10a–c, the solutions of these compounds exhibit strong NLO absorptions from 430 to 480 nm with the strongest NLO absorption observed at 430 nm for all compounds. At 430 nm, when the incident fluence reaches 0.25 J/cm$^2$, the transmittance is 63% for **6**, and 54% for **7** and **8**. In contrast to the disubstituted bithiophenes, **2**, **3**, and **4**, in which the NLO absorption clearly increases in the order Se > S > O, only small differences are observed in the nonlinear transmittances of the monosubstituted bithiophenes with different X groups (**6**, **7** and **8**). The saturated solutions of compounds **6** and **7** showed some decomposition beginning at an incident fluence of approximately 0.6 J/cm$^2$. This may be due to the strong absorption of laser by the highly concentrated solutions resulting in rapid heating even though the laser repetition rate is only 10 Hz. Measurement of the power limiting performance at higher fluences will require the use of single laser shots.


dx.doi.org/10.1021/ic201309k | *Inorg. Chem.* 2012, 51, 2016–2030

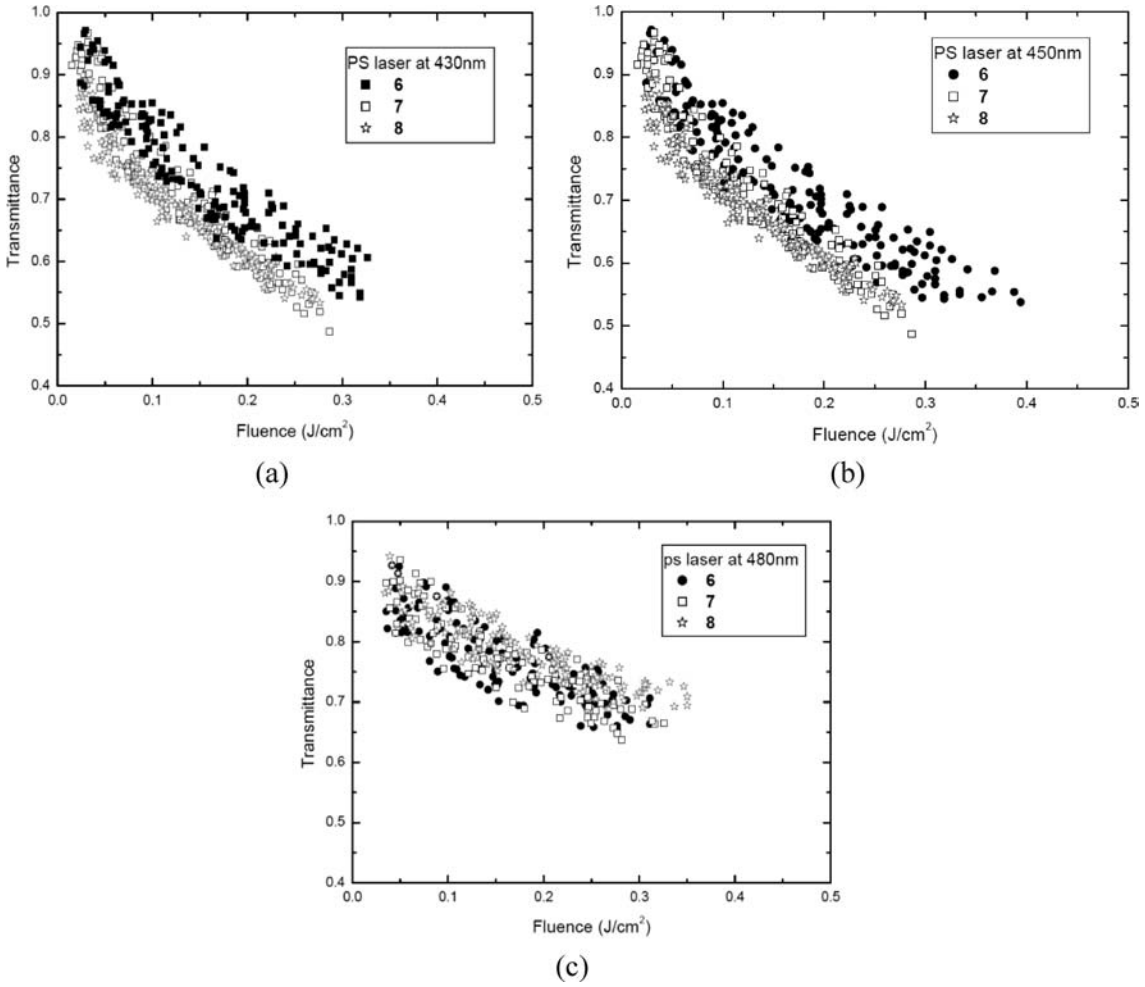


**Figure 10.** Comparison of the nonlinear transmittances of $CHCl_3$ solutions of **6**–**8** at the same concentration of 1.66 M in a 1-mm cell with 27 ps laser pulses at (a) 430, (b) 450, and (c) 480 nm.

## CONCLUSIONS

A series of bithiophene derivatives that are either symmetrically disubstituted or monosubstituted with $Ph_2(X)P$ (X = O, S, Se) groups have been synthesized, and the X-ray crystal structures of four of the compounds have been determined. Their linear optical properties have been evaluated using electronic absorption and fluorescence spectroscopy, and their third-order NLO properties have been evaluated using nonlinear transmission measurements at wavelengths between 430 and 480 nm with picosecond laser pulses.

The fluorescence studies demonstrate that the emission maxima and quantum yields of the $Ph_2(O)P$-substituted bithiophenes are much higher than that of bithiophene with the quantum yields of $Ph_2(O)P(C_4H_2S)_2H$, $Ph_2(O)P(C_4H_2S)_2P(O)Ph_2$, $Ph_2(O)P(C_4H_2S)_2CO_2Me$, and $Ph_2(O)P(C_4H_2S)_2CH_2OH$ increased by factors of 13, 14, 14, and 22, respectively, relative to that of bithiophene. The quantum yields of the $Ph_2P(X)$-substituted bithiophenes are generally higher than are those of the terthiophene analogues with the same substituents even though the quantum yield of bithiophene is much lower than that of terthiophene (0.012 versus 0.059). The DFT studies provide insight into the manner in which changes in the structures affect the fluorescence and suggest that fluorescent materials with even higher quantum efficiencies could be developed by judicious choices of substituents on the $Ph_2P(O)$-substituted bithiophenes. The bithiophene derived materials have the added advantages that they can be prepared in high yields from inexpensive and commercially available bithiophene, and they are more soluble and more easily processed than are those derived from higher oligothiophenes.

Third-order NLO studies demonstrate that members of this family of compounds exhibit high linear transmission but strong nonlinear absorption in the violet-blue spectral region from 430 to 480 nm, and that both extent of the nonlinear absorption and the maximum wavelength at which the nonlinear absorption occurs can be tuned by varying the groups attached to the phosphorus and the substituents on the bithiophene. Saturated chloroform solutions of the monosubstituted bithiophenes, $Ph_2(O)P(C_4H_2S)_2H$ and $Ph_2(S)P(C_4H_2S)_2H$, exhibit the best NLO absorption of picosecond laser pulses that has been reported, and thus these compounds are promising candidates for use in broadband optical power limiters.

## ASSOCIATED CONTENT

### Supporting Information

Crystals structure data for **4**, **6**, **7**, and **10**, including tables of atomic coordinates, anisotropic thermal parameters, all bond lengths and angles, and hydrogen isotropic displacement parameters using the crystallographic information file (CIF) format. This material is available free of charge via the Internet at http://pubs.acs.org.


dx.doi.org/10.1021/ic201309k | *Inorg. Chem.* 2012, 51, 2016–2030

## AUTHOR INFORMATION


### Corresponding Author

*Tel: (205) 934-8294. Fax: (205) 934-2543. E-mail: gmgray@uab.edu (G.M.G.); qzhao551@gmail.com (Q.Z.).


## ACKNOWLEDGMENTS


The authors gratefully acknowledge an Army Research Laboratories Cooperative Agreement (W011NF-06-2-0033) and NSF Cooperative Agreements (EPS-0814103 and EPS-0903787) for support of this research.


## REFERENCES


(1) Sun, S.; Dalton, L. R. *Introduction to Organic Electronic and Optoelectronic Materials and Devices*; CRC Press, Taylor & Francis Group: Boca Raton, FL, 2008.

(2) Interrante, L. V.; Hampden-Smith, M. J. *Chemistry of Advanced Materials: An Overview*; Wiley-VCH: New York, 1998.

(3) Denk, W.; Strickler, J. H.; Webb, W. W. *Science* **1990**, *248*, 73.

(4) Strickler, J. H.; Webb, W. W. *Opt. Lett.* **1991**, *16*, 1780.

(5) Maruo, S.; Nakamura, O.; Katawa, S. *Opt. Lett.* **1997**, *22*, 132.

(6) Cumpston, B. H.; Ananthavel, S. P.; Barlow, S. *Nature* **1999**, *51*, 398.

(7) Spangler, C. W. *J. Mater. Chem.* **1999**, *9*, 2013−2020.

(8) Hales, J. M.; Zheng, S.; Barlow, S.; Marder, S. R.; Perry, J. W. *J. Am. Chem. Soc.* **2006**, *128*, 11362−11363.

(9) Zieba, R.; Desroches, C.; Chaput, F.; Carlsson, M.; Eliasson, B.; Lopes, C.; Lindgren, M.; Parola, S. *Adv. Funct. Mater.* **2009**, *19*, 235−241.

(10) Lin, T.-C.; Chen, Y.-F.; Hu, C.-L.; Hsu, C.-S. *J. Mater. Chem.* **2009**, *19*, 7075−7080.

(11) Lin, T.-C.; He, G.-S.; Zheng, Q.-D.; Prasad, P. N. *J. Mater. Chem.* **2006**, *16*, 2490−2498.

(12) Lin, T.-C.; He, G.-S.; Prasad, P. N.; Tan, L.-S. *J. Mater. Chem.* **2004**, *14*, 982−991.

(13) Rumi, M.; Barlow, S.; Wang, J.; Perry, J. W.; Marder, S. R. *Adv. Polym. Sci.* **2008**, *213*, 1−95.

(14) Barlow, S.; Marder, S. R. *Funct. Org. Mater.* **2007**, 393−437.

(15) Marder, S. R. *Chem. Commun.* **2006**, *2*, 131−134.

(16) Belfield, K. D.; Yao, S.; Bondar, M. V. *Adv. Polym. Sci.* **2008**, *213*, 97−156.

(17) Belfield, K. D.; Schafer, K. J.; Liu, Y.; Liu, J.; Ren, X.-B; Van Stryland, E. W. *J. Phys. Org. Chem.* **2000**, *13*, 837−849.

(18) Bhawalkar, J. D.; He, G. S.; Prasad, P. N. *Rep. Prog. Phys.* **1996**, *59*, 1041−1070.

(19) Charlot, M.; Izard, N.; Mongin, O.; Riehl, D.; Blanchard-Desce, M. *Chem. Phys. Lett.* **2006**, *417*, 297−302.

(20) Charlot, M.; Porres, L.; Entwistle, C. D.; Beeby, A.; Marder, T. B.; Blanchard-Desce, M. *Phys. Chem. Chem. Phys.* **2005**, *7*, 600−606.

(21) Silly, M. G.; Porres, L.; Mongin, O.; Chollet, P.-A.; Blanchard-Desce, M. *Chem. Phys. Lett.* **2003**, *379*, 74−80.

(22) Mongin, O.; Brunel, J.; Porres, L.; Blanchard-Desce, M. *Tetrahedron Lett.* **2003**, *44*, 2813−2816.

(23) Morel, Y.; Irimia, A.; Najechalski, P.; Kervella, Y.; Stephan, O.; Baldeck, P. L. *J. Chem. Phys.* **2001**, *114*, 5391−5396.

(24) Zhao, Q.; Wang, J.; Freeman, J. L.; Murphy-Jolly, M.; Wright, A. M.; Scardino, D. J.; Hammer, N. I.; Lawson, C. M.; Gray, G. M. *Inorg. Chem.* **2011**, *50*, 2015−2027.

(25) Zhao, Q.; Owens, S. B. Jr.; Gray, G. M.; Wang, J.; Lawson, C. M. *Main Group Chem.* **2007**, *6*, 215−229.

(26) Wang, J.; Zhao, Q.; Lawson, C. M.; Gray, G. M. *Opt. Commun.* **2011**, *284*, 3090−3094.

(27) Stott, T. L.; Wolf, M. O. *J. Phys. Chem. B* **2004**, *108*, 18815−18819.

(28) Field, J. S.; Haines, R. J.; Lakoba, E. I.; Sosabowski, M. H. *J. Chem. Soc., Perkin Trans. I* **2001**, 3352−3360.

(29) *CAD4-PC*, version 1.2; Enraf-Nonius: Delft, The Netherlands, 1988.

(30) Sheldrick, G. M. *SHELXTL NT*, version 6.12; Bruker AXS, Inc.: Madison, WI, 2001.

(31) Lakowicz, J. R. *Chapter 2, Principles of Fluorescence Spectroscopy*, 2nd ed.; Springer Science + Business Media Inc.: New York, NY, 2004.

(32) Adams, M. J.; Highfield, J. G.; Kirkbright, G. F. *Anal. Chem.* **1977**, *49*, 1850−1852.

(33) *Spartan'08*; Wavefunction, Inc.: Irvine, CA, 2008.

(34) Padmaperuma, A. B.; Sapochak, L. S.; Burrows, P. E. *Chem. Mater.* **2006**, *18*, 2389−2396.

(35) Frisch, M. J.; Trucks, G. W.; Schlegel, H. B.; Scuseria, G. E.; Robb, M. A.; Cheeseman, J. R.; Montgomery, Jr., J. A.; Vreven, T.; Kudin, K. N.; Burant, J. C.; Millam, J. M.; Iyengar, S. S.; Tomasi, J.; Barone, V.; Mennucci, B.; Cossi, M.; Scalmani, G.; Rega, N.; Petersson, G. A.; Nakatsuji, H.; Hada, M.; Ehara, M.; Toyota, K.; Fukuda, R.; Hasegawa, J.; Ishida, M.; Nakajima, T.; Honda, Y.; Kitao, O.; Nakai, H.; Klene, M.; Li, X.; Knox, J. E.; Hratchian, H. P.; Cross, J. B.; Bakken, V.; Adamo, C.; Jaramillo, J.; Gomperts, R.; Stratmann, R. E.; Yazyev, O.; Austin, A. J.; Cammi, R.; Pomelli, C.; Ochterski, J. W.; Ayala, P. Y.; Morokuma, K.; Voth, G. A.; Salvador, P.; Dannenberg, J. J.; Zakrzewski, V. G.; Dapprich, S.; Daniels, A. D.; Strain, M. C.; Farkas, O.; Malick, D. K.; Rabuck, A. D.; Raghavachari, K.; Foresman, J. B.; Ortiz, J. V.; Cui, Q.; Baboul, A. G.; Clifford, S.; Cioslowski, J.; Stefanov, B. B.; Liu, G.; Liashenko, A.; Piskorz, P.; Komaromi, I.; Martin, R. L.; Fox, D. J.; Keith, T.; Al-Laham, M. A.; Peng, C. Y.; Nanayakkara, A.; Challacombe, M.; Gill, P. M. W.; Johnson, B.; Chen, W.; Wong, M. W.; Gonzalez, C.; Pople, J. A. *Gaussian 03*, revision C.02; Gaussian, Inc.: Wallingford CT, 2004.

(36) Liu, Y.-L.; Feng, J.-K.; Ren, A.-M. *J. Phys. Chem. A* **2008**, *112*, 3157−3164.

(37) Li, Z.-H.; Wong, M.-S.; Fukutani, H.; Tao, Y. *Chem. Mater.* **2005**, *17*, 5032−5040.

(38) Mori, N.; Togo, H. *Tetrahedron* **2005**, *61*, 5915−5925.

(39) Andersen, N. G.; Keay, B. A. *Chem. Rev.* **2001**, *101*, 997−1030.

(40) Verkade, J. G.; Quin, L. D., Ed. *Phosphorus-31 NMR Spectroscopy in Stereochemical Analysis*; VCH Publishers: Deerfield Beach, FL, 1987.

(41) Allen, D. W.; Taylor, B. F. *J. Chem. Soc., Dalton Trans.* **1982**, 51.

(42) Létard, J. F.; Guionneau, P.; Codjovi, E.; Lavastre, O.; Bravic, G.; Chasseau, D.; Kahn, O. *J. Am. Chem. Soc.* **1997**, *119*, 10861−10862.

(43) Létard, J. F.; Guionneau, P.; Rabardel, L.; Howard, J. A. K.; Goeta, A. E.; Chasseau, D.; Kahn, O. *Inorg. Chem.* **1998**, *37*, 4432−4441.

(44) Wesolek, M.; Meyer, D.; Osborn, J. A.; De Cian, A.; Fisher, J.; Derory, A.; Logoll, P.; Drillon, M. *Angew. Chem., Int. Ed. Engl.* **1994**, *33*, 1592.

(45) Skoog, D. A.; Holler, F. J.; Crouch, S. R. *Principles of Instrumental Analysis*, 6th ed.; Thomson Brooks/Cole: Pacific Grove, CA, 2007; pp 399.

(46) Becker, R. S.; Seixas de Melo, J.; Macuanita, A. L.; Elisei, F. *J. Phys. Chem.* **1996**, *100*, 18683−18695.

(47) Lukes, V.; Aquino, A.; Lischka, H. *J. Phys. Chem. A* **2005**, *109*, 10232−10238.

(48) Valeur, B. *Molecular Fluorescence: Principles and Applications*; Wiley-VCH: Weinheim, Germany, 2002.

(49) Henari, F.; Callaghan, J.; Stiel, H.; Blau, W.; Cardin, D. J. *Chem. Phys. Lett.* **1992**, *199*, 144−148.